Semiconductors in Industrial Waste Heat Collection Improvements

by

David Walden

A Thesis Submitted in Partial Fulfillment of the Requirements for the Degree

Master of Science

Major Subject: Engineering

West Texas A&M University

Canyon, Texas

August 2021

Abstract

Thermoelectric generators (TEGs) use the Seebeck effect to transform thermal flow into electrical potential, have no moving parts, are low maintenance, have a long material life, and can be readily serviced. Utilizing these principles in conjunction with heat transfer manipulation, TEGs could be utilized as a new avenue for energy recovery. A cubical system was built with TEGs within the walls of the structure. The top was covered with standard building materials to simplify the proof of concept. The inside was then heated to be approximately 30˚C with manipulation of the thermal conductance of the cover of the system. The heat recovery is ~40mW for the control case and ~50 mW for the experimental case. Using the regression model indicates, based on the improvement in energy recovery, that this technology and approach can be implemented on a greater scale to produce the desired result of increased energy savings, through increased energy recovery. The results of the study netted some sporadic data so a much simpler system was tracked. This simple system in conjunction with the other collected data showed an improvement of power production. The relationship between the suppression and the generation is related to the ratio changes of thermal fluxes throughout the system.

Signature Page

Committee Chair: **Roy Issa, PhD**

 Date 06/24/21

Committee Member: **Kenneth Leitch, PhD**

 Date 06/24/21

Committee Member: **Emad Manla, PhD**

 Date 06/24/21

Associate Dean: **Pamela Lockwood-Cooke, PhD**

_____ Date_____

CoE Dean: **Emily Hunt, PhD**

_____ Date _____

Graduate School Dean: **Angela Spalding, PhD**

_____ Date _____

Acknowledgements

I would like to acknowledge the effort put forth by the graduate committee in times when communication and progress were difficult. The funding to pursue this research is from a Killgore grant from West Texas A&M University. I would also like to acknowledge the contributions of the College of Engineering. I would like to thank the committee individually of Dr. Roy Issa, Dr. Emad Manla, and Dr. Kenneth Leitch.

Table of Contents

Abstract ii

Signature Page iii

Acknowledgements iv

Table of Contents v

Table of Figures vii

Table of Tables ix

Nomenclature x

1.Introduction 1

2.Literature Review 3

3.Theory 9

3.1. Heater Module 9

3.2. Inner Chamber Heat Transfer 11

3.2.1. Octant 1-4 11

3.2.2. Octant 5-8 13

3.2.3. Top/Bottom Thermal Resistance loop 14

3.2.4. Thermal electric conversion circuit 17

3.3. Power Generation Circuit 18

3.4. Combined system 21

4.Experimental System 24

5.Simulations 26

5.1. Simple Simulation 26

5.2. Simulation Based on Redesign 29

6.Experimental Results 34

7.Conclusions 40

8.Reference 42

Table of Figures

FIGURE 1. RESULTING DATA PLOT REPLICATED FROM STUDY[3]. 4

FIGURE 2. PREVIOUS DESIGNS. NEW DESIGNS. REPRODUCED FROM 5

FIGURE 3. THE TEST SYSTEM IN THE "COGENERATION STUDY" REPRODUCED FROM 6

FIGURE 4. ELECTRICAL HEATER CIRCUIT 10

FIGURE 5. THIS IS THE OCTANT CIRCUIT DIAGRAM. EACH LINE REPRESENTS A PARALLEL CIRCUIT EACH PARALLEL LINE REPRESENTS A SERIES CIRCUIT. 13

FIGURE 6. LOWER OCTANT SCHEMATIC SHOWING OCTANT 5 14

FIGURE 7 NON- INSULATED WALL THERMAL CIRCUIT 15

FIGURE 8. INSULATED WALL THERMAL CIRCUIT. 15

FIGURE 9. ELECTRICAL EQUIVALENT OF THE THERMAL CIRCUIT 16

FIGURE 10. THERMAL ELECTRIC CONVERSION CIRCUIT 18

FIGURE 11. ARDUINO CIRCUIT DRAWING 19

FIGURE 12. DIGITAL DRAWING OF THE ARDUINO CIRCUIT CONNECTED WITH THE TEGS 20

FIGURE 13. TEG CIRCUIT DIAGRAM 20

FIGURE 14. FULL THERMAL ELECTRIC CIRCUIT 22

FIGURE 15. FULL THERMAL ELECTRIC CIRCUIT WITH EXPANDED COMPONENTS 23

FIGURE 16. NON-INSULATED SYSTEM 24

FIGURE 17. INSULATED SYSTEM WITH MATERIAL SHOWING 25

FIGURE 18. SIMULATION SET-UP OF STANDARD SYSTEM(LEFT) AND MODIFIED INSULATED SYSTEM(RIGHT). 27

FIGURE 19 THE SIMULATED STEADY STATE SIGNAL OF BOTH CASE 1 AND CASE 2 28

FIGURE 20 THE EFFICIENCY CHANGE BASED ON THE SYSTEM BEING UTILIZED..... 29
FIGURE 21. REDESIGNED SIMULATION SETUP 30
FIGURE 22. TILE NON-INSULATED SYSTEM 31
FIGURE 23 TILE INSULATED SYSTEM..... 31
FIGURE 24. NON-INSULATED SYSTEM 32
FIGURE 25. INSULATED SYSTEM 4 CELL VOLTAGE PRODUCTION 32
FIGURE 26. INSULATED SYSTEM TEMPERATURE PLOT..... 34
FIGURE 27. CONTROL SYSTEM TEMPERATURE PLOT..... 35
FIGURE 28. POWER GENERATION OF CASE 1 AND CASE 2..... 37
FIGURE 29. POWER GRAPH FOR TRANSIENT CONDITIONS 37
FIGURE 30. POWER TEG 1 CELL VERSUS INSULATED TEG..... 38
FIGURE 31. POWER GENERATION TEG CELL - 1 TILE VERSUS INSULATED TILE THROUGH TIME .. 39

Table of Tables

TABLE 1 MATERIAL PROPERTIES OF THE SYSTEM[9][3][6] 35

TABLE 2. SYSTEM GEOMETRIC PROPERTIES 36

Nomenclature

Symbol	Units	Representation
T_h	$\text{Kelvin}(\text{K})$	High Temperature of the System
R_L	$\text{Ohms}(\Omega)$	Resistance of the System
I	$\text{Ampere}(\text{A})$	Current of the circuit
E	$\text{Joule}(\text{J})$	Energy
ΔT	$\text{Kelvin}(\text{K})$	Temperature Difference across the boundary
Z	K^{-1}	Figure of Merit
T_{avg}	$\text{Kelvin}(\text{K})$	Average Temperature
R_{th}	$\text{Ohms}(\Omega)$	Thevenin Resistance of tiles
K_s	$\frac{\text{W}}{(m^2 \cdot K)}$	Thermal Conductivity
U	$\frac{(m^2 \cdot K)}{\text{W}}$	Thermal Conductance
$\dot{Q}$	$Watts(\text{W})$	Heat Flow
V	m^3	Volume
C_v	$\frac{kJ}{(kg \cdot k)}$	Heat Capacity at Constant Volume
C_p	$\frac{kJ}{(kg \cdot k)}$	Heat Capacity at Constant Pressure

1. Introduction

In both industrial and residential energy applications, waste heat often accounts for a disproportionate share of the energy losses. Thermoelectric generators (TEGs) are useful semiconductor devices that operate based upon a phenomenon called the Seebeck effect. This is part of a larger relationship called the thermoelectric effect, which correlates the contributions of William Thomson, Johann Seebeck, and Jean Peltier[1]. TEGs convert heat flux across a boundary and cause work to be imparted on electrons. This work produces electrical potential, which can be used, much in the same way as a battery. TEGs are solid-state devices that do not require any fluids for fuel or cooling, making them non-orientation dependent. These characteristics allow for a variety of uses such as: zero-gravity and deep-sea applications [2], and any control volume in which a temperature gradient exists between an internal boundary layer. This power generation is achieved passively; thus, the primary generation operation is independent of the operation conditions of the tertiary system. The flexible applications, resulting from these properties, allow for TEGs to be implemented in creative ways.

The potential creative applications of TEGs is of specific interest in industrial energy conservation practices, due to their capability to remedy the outsized heat losses. This approach also generates a potential for hybridized systems which have higher efficiencies than their homogeneous counterparts. The option to use the waste energy and, to some degree, isolate the plant operation from the main line operation[3] is a

viable one. Other alternatives such as utilizing the recaptured energy for purposes aside from the tertiary system are also feasible. Several obstacles are encountered when using standard approaches to recapture waste heat, such as:

- Temperature limits and cost of recovery equipment.
- Low-grade waste heat (when waste heat exists at a low temperature difference compared to the ambient).
- Difficulty of recovering waste heat from sources not considered such as:

1. Efficient Electronics
2. Efficient Housing
3. TEG embedded materials

The generators are perfect to address heat loss phenomena by a physical process called the Seebeck Effect, which is a conversion of thermal energy to electrical energy. This would occur in a way that would be economically significant if properly implemented. TEGs are often seen as a novelty but are assumed to lack practical application due to limited progress made on improving the Figure of merit (Z) which is defined as the ratio of the Seebeck Effect squared and Thermal Diffusivity. In the non-transient case this relationship simplifies to be a ration of the Seebeck Coefficient squared and the Thermal Conductance. This lack of Z score improvement often leads to a misconception involving the low maximum theoretical efficiency, which is 5.4% [4], [5] of the available heat loss. This could seem like a low performance but given its use as efficiency booster rather than a mainline generation system provides many advantages to its use.

2. Literature Review

A review of current academic literature was implanted to ensure that a new approach was being considered. This first started with verifying the behavior of individual TEGs. In the study, "Thermoelectric Power Generation Using Waste-Heat Energy as an Alternative Green Technology," an assertion of tiered Peltier module stack is considered.[3] The hypothesis is that the system can be improved upon by introducing these tiered systems. The study designs a set up in which the largest tile area is directly contacting the heated surface, and the progressively smaller tiles are stacked centered directly above. The resulting data plot from this study shows the expected behavior, Figure 1 (page 5) each of the tiled surface. Thus, to validate our findings the early ramp up values should have a "similar" shape. This does not mean the same, however, due to the other electronic components the behavior will deviate as time passes and then will be bound by the internal temperature, but the positive correlation should hold.

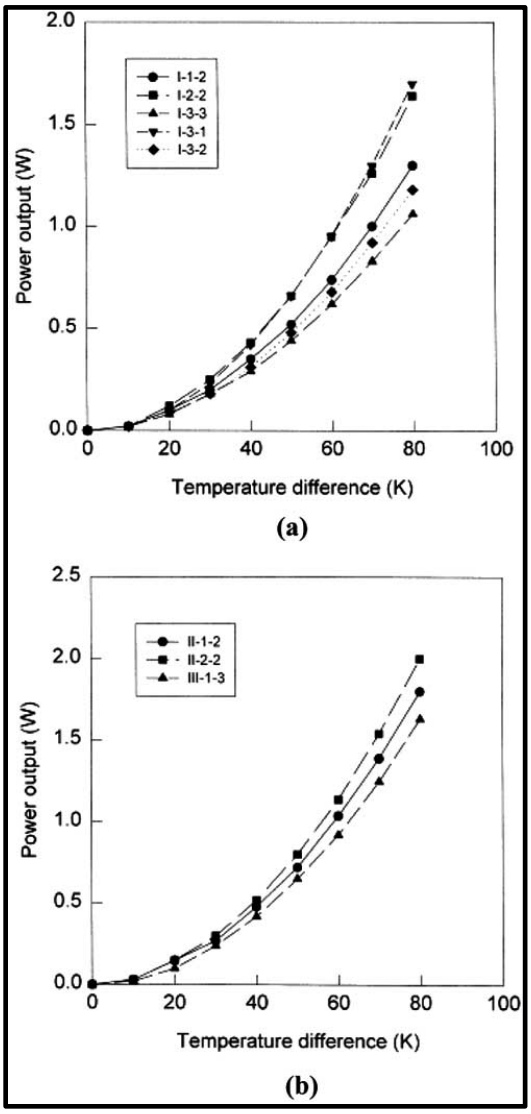

Figure 1. Resulting Data Plot replicated from study[3].

In, "A potential candidate for the sustainable and reliable domestic energy generation- Thermoelectric cogeneration system," an approach with similar consideration that had originally been proposed for this study were presented. This approach considered the outflow piping from the heat source, however, instead of directly connecting to a boiler wall. This was asserted to produce a higher output of electrical than the current location. Thus, the use of transport system with higher temperatures can also be established in conjunction with the use of such systems on walled surfaces. The

formerly observed system and the proposed new system are shown in Figure 2. This would utilize a preheater arrangement and would also require thermal radiation input. The mixed case creating several intertwined tertiary systems is what was experimented.

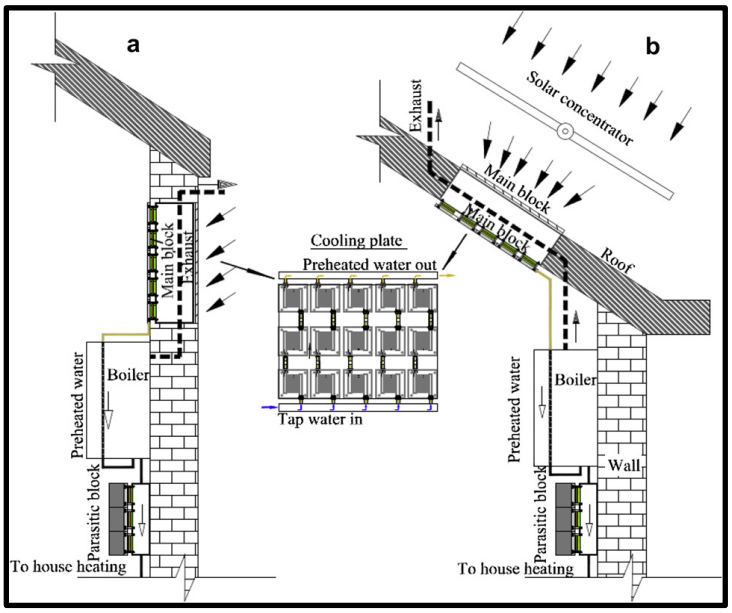

Figure 2. Previous Designs. New Designs. Reproduced from [6]

This resulted in a system that was constructed that pushed heated water through a TEG cladded pipe and tracked the electrical output the schematic is shown below in Figure 3.

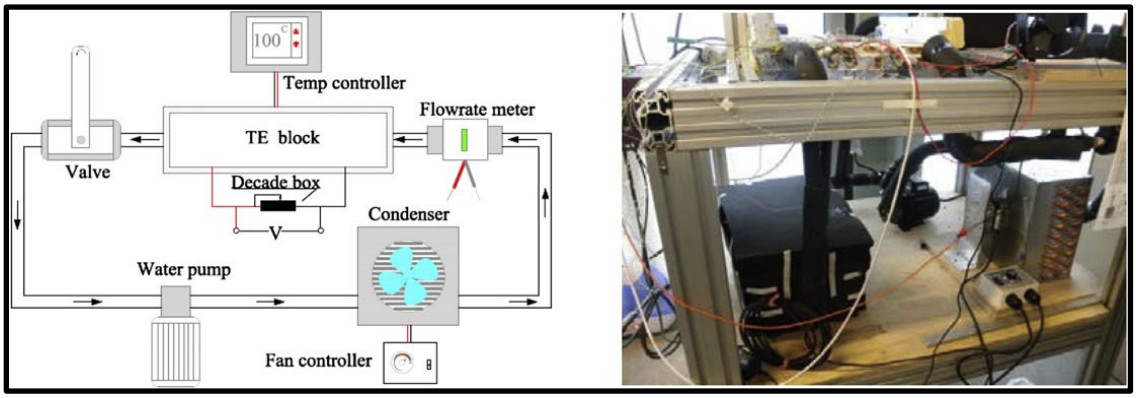

Figure 3. The Test System in the "Cogeneration Study" reproduced from [6]

The conclusion drawn shows that such a system would be viable and lower the net embodied carbon by raising the total energy production. Thus, it is shown the viability of TEGs previously and also the newer system could further generate a higher generation.

The study, 'Effect of micro-channel geometry on fluid flow and mixing,' uses a method of fluid flow in which through subtle geometric changes fluid flow can be manipulated in the same way that electricity is manipulated.[7] The approach can really best describe the way a logic machine works. If we consider that the constants used in thermoelectric generation as probabilities of heat flowing through, then if we increase a probability of heat flow through one port then we can decrease heat flow through another port such that the input and the outputs are equivalent when they are summed but one of the outputs will receive a lower magnitude of the sum.

In, Heat Convection, the mathematics of the Convection are considered.[8] This directs the convection as Navier Stokes equation and assume constant pressure. Using vector calculus, a result is generated, and the output is given using various geometric relationships. A similar consideration for the final representation of the complexed thermo-electric circuit.

Given the consideration of manipulating geometry the first consideration was the thickness, however, without any ability to manufacture TEGs this approach was instead looked into from the literature perspective. The study proposed a complete redesign of thermoelectrics that where thinner than the currently implemented. It was found that these would as well as the standard with standard TEGs with miner design consideration being made at the small scale causing hard to control geometries. This, however, is based on the acknowledgement that by making a thinner component you increase the thermal conductance thus decreasing the Figure of merit (Z)[9].

In the PhD Dissertation, by Yuri M. Zuev, a nano scale experiment using nano wires is created to observe the nanoscale thermoelectric transport.[10] This helps to better understand the way that thermo electric transport works and thus helps to better consider within the system. This will allow for a more advanced relationship with the thermo electric generators be established in the document's theory section. It is discovered based upon the materials he is working with that these are not suitable candidates for these Nanoscale materials. The text discussed the mathematics of the micro and nano scale TEGs from a pure mathematics perspective. It is shown that the relationship is thought to be a tensor of the flux through the wall. This has basis in reality given the relationship of heat and electricity to other physical phenomenon. [5]

The electrical optimization first considered a potential for back flow. It was discovered through a website called, "electronics hub," that diodes can be used to prevent backflow. It was also considered how to exchange the voltage and current to reuse the energy in the circuit to keep it powered even after the power was off. This, however, was abandoned due to the layer of complexity added to tuning the system.[11] The buck-boost was the component considered and this operates by using a switch and that introduces a

duty cycle to the output line. This duty cycle then math mathematically introduces momentum into the circuit which is produced by the constriction of the input and then sudden relieve of that constriction.[12] [13]. Thus, when designing the thermo-electric circuit tuning the electrical parameters must include the estimated voltage drop across the diode. These were shown to be piece wise with a minimum drop defined as parameter of the diode. To avoid complications the diode was considered a resistor in all future calculations but will be picked such that the voltages production overcomes the voltage drop.

3. Theory

The theory is best approached using modules. For the purposes of consistency, the analogous methods of the electrical system and mechanical system are implemented. The modular electrical and mechanical control volumes are connected by nodes that act as a "black box" conversion circuit. This allows us to treat each connecting node as if it were simply a current dividing circuit. This allows for tuning of the output power optimization and the tuning the thermal conductance.

3.1. Heater Module

The first electrical module is the electrical heater and Arduino microcontroller power circuit. This is used to heat the chambers and also to take measurements. These measurements are taken through manipulation of the voltage flows to leak a small amount of power to this component of the circuit. The microcontroller is programmed to take these measurements and transmit them to another microcontroller. These values are transmitted to an external PC called a Raspberry Pi. The Raspberry Pi B can be used with a few lines of code to read the data and write to CSV file. While these concepts are interesting the actual data transmission losses will be neglected and thus any communication beyond the initial value voltage readings would be unnecessary. Some of the simple considerations are the voltage drops across the Arduinos and the voltage inputs of the Arduinos. This can be simplified further if a voltage regulator is introduced in the circuit. This allows one to only consider the first loop while holding the second

loop as directly correlated and thus the circuit will behave predictably. In Figure 4, the circuit is shown using Simulink for clear and easily interpreted examples.

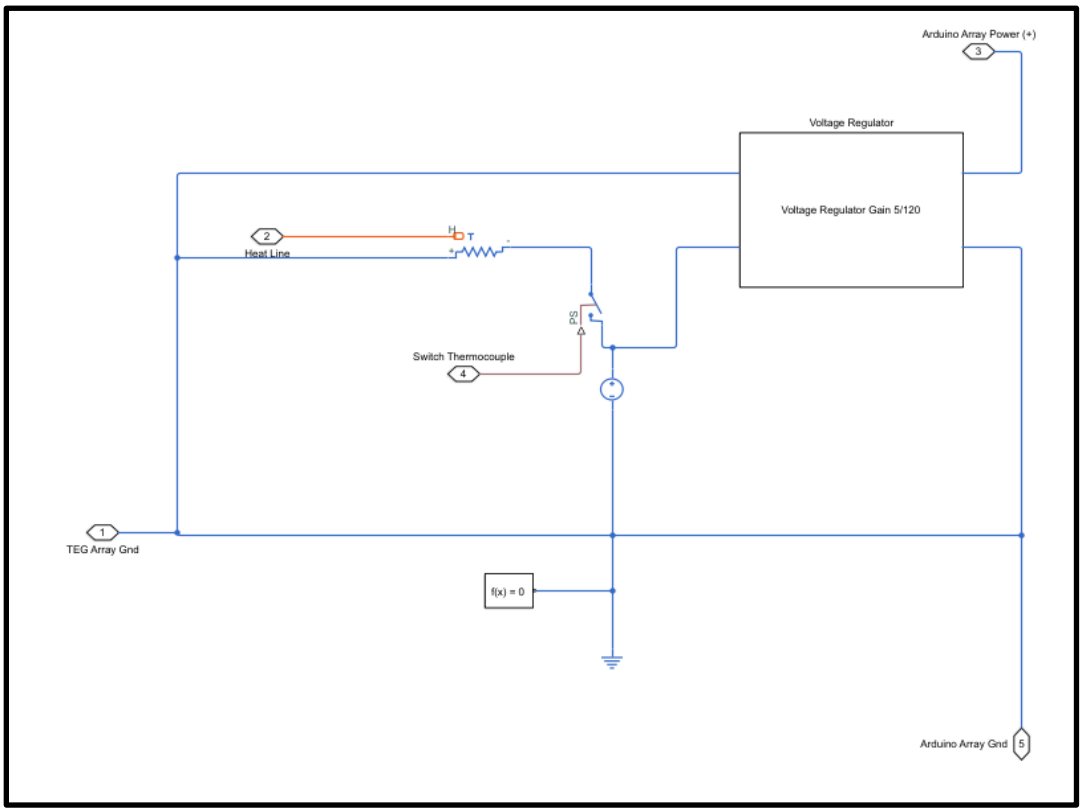

Figure 4. Electrical Heater Circuit

The loop that should be considered is the loop for the heater as this will be the only time in which a heat momentum input is experienced. It can be quickly discerned that the power rating for the heater will be met for the system to turn on and thus the first loop will follow the behavior in equation 1.

$$P_{in} = \frac{1}{2} I^2 R_0 T(t) \tag{1}$$

This allows us to relate our power input to the circuit. While this is a simple circuit and thus the components are easy to discern if a more complicated system is considered or to optimize the power to run the microcontroller further optimization can be considered. However, by assuming a power consumption of the heating element (60 W), the

additional loops can be neglected and ignored from a power input perspective. The node of Thermo-electric relationship, caused by the heater, is shown in equation 2.

$$0 = K\left(t_c\right)\ddot{T} + \frac{1}{2}\left(R_0^2 + K_{out}\right)\dot{T} \tag{2}$$

As we have previously asserted the equation is written with appropriate representation for the power input to find a relationship between the differential equations. The voltage drop across the Arduino circuit is the same as the voltage drop across the heating element with the voltage regulator acting as to reduce the voltage. This works like a boost buck converter and acts as an increase to the input current and a decrease to the voltage. The current is then decreased by powering the microcontroller in parallel.

3.2. Inner Chamber Heat Transfer

In the inner chamber the shell thermal circuit was considered first. This employed the use of symmetry in separated octants of the system. The energy balance for heat transfer were divided into two types of octants. Each Octant has an initial heat flux from the temperature potential across the boundary. This allowed for a simple relationship between the input variables and the output. An important but relevant consideration is that quadrants containing the Octants $n, \left(O_n\right)$ and $\left(n+4\right), \left(O_{n+4}\right)$ are not symmetric, but rather the quadrants are symmetric with one another.

3.2.1. Octant 1-4

Octant 1-4 receive a heat flux of magnitude related to the previous equation. To appropriately engage this conceptually a balance between the heat out should match the heat in the air volume elements of each octant. This is shown in the relationship below.

$$\begin{aligned} q_{in} &= q_1 + q_2 + q_3 + q_4 \\ q_{in} &= h_1\Delta T_1 + h_2\Delta T_2 + h_3\Delta T_3 + h_4\Delta T_4 \\ \Delta T &= \Delta T_1 = \Delta T_2 = \Delta T_3 = \Delta T_4 \\ q_{in} &= \left(h_1 + h_2 + h_3 + h_4\right)\Delta T \end{aligned}$$

Now if we consider the change in temperature with respect to time, we get the relationship in equation 3

$$\dot{q}_{in} = \left(h_1 + h_2 + h_3 + h_4\right)\dot{T} \tag{3}$$

Now recall that the heat in is dictated by the previous differential equation. Next an energy balance on the octant 1 shell is performed.

$$\dot{E}_{stored} = \dot{E}_{in} - \dot{E}_{out}$$

$$\dot{E}_{abs_1} + \dot{E}_{teg_1} + \dot{E}_{abs_{16}} + \dot{E}_{teg_{16}} + \dot{E}_{air} = \dot{q}_{in,1} - \left(\dot{q}_{\mathrm{abs}_1} + \dot{q}_{\mathrm{teg}_1} + \dot{q}_{\mathrm{abs}_{16}} + \dot{q}_{\mathrm{teg}_{16}} + \dot{q}_{roof_1} + \dot{q}_{O_{1-5}}\right)$$

$$\dot{E} = \rho c V \ddot{T}$$

$$\dot{q}_{con} = H\dot{T} \quad where\ H = hA$$

Introducing the relevant relationships results in the output shown in equation 4.

$$0 = \dot{q}_{in,1} - \left(2k\dot{T}_{teg} + 2k\dot{T}_{abs} + \mathrm{H}_{O_{1-5}}\dot{T}_{air} - K\dot{T}_{abs}\right) - \left(2\left(\rho cV\right)_{abs}\ddot{T}_{abs} + 2\left(\rho cV\right)_{teg}\ddot{T}_{teg} + \left(\rho cV\right)_{air}\ddot{T}_{air}\right)$$

$$\dot{q}_{in,1} = \left(2k\dot{T}_{teg} + 2k\dot{T}_{abs} + \mathrm{H}_{O_{1-5}}\dot{T}_{air} + K\dot{T}_{abs}\right) + \left(2\left(\rho cV\right)_{abs}\ddot{T}_{abs} + 2\left(\rho cV\right)_{teg}\ddot{T}_{teg} + \left(\rho cV\right)_{air}\ddot{T}_{air}\right) \tag{4}$$

Using Figure 5 for the abs allows for a single loop being generated.

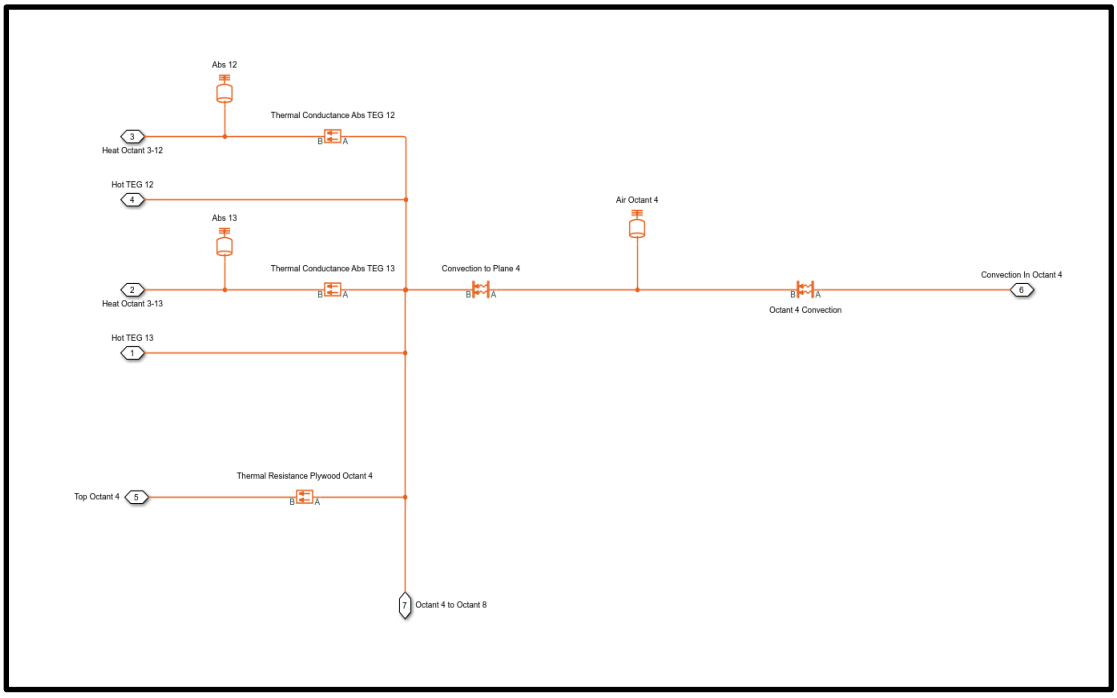

Figure 5. This is the octant Circuit diagram. Each line represents a parallel circuit each parallel line represents a series circuit.

The abs line will be a similar approach but will only consider the main line and results in equation 5.

$$\left(\rho cV\right)_{Abs}\ddot{T}_{air} = \mathrm{H}_{O_1}\dot{T}_{air} - K\dot{T}_{abs} \tag{5}$$

Each octant will have terms that are similar with the only distinction made being the flux at the input nodes being flux for the first 4 octants.

3.2.2.Octant 5-8

In octant 5-8 shown in Figure 6. Using the same approach as Octants 1-4 a set of correlation for the Octants 5-8 can also be asserted. This energy balance technique used previously result in

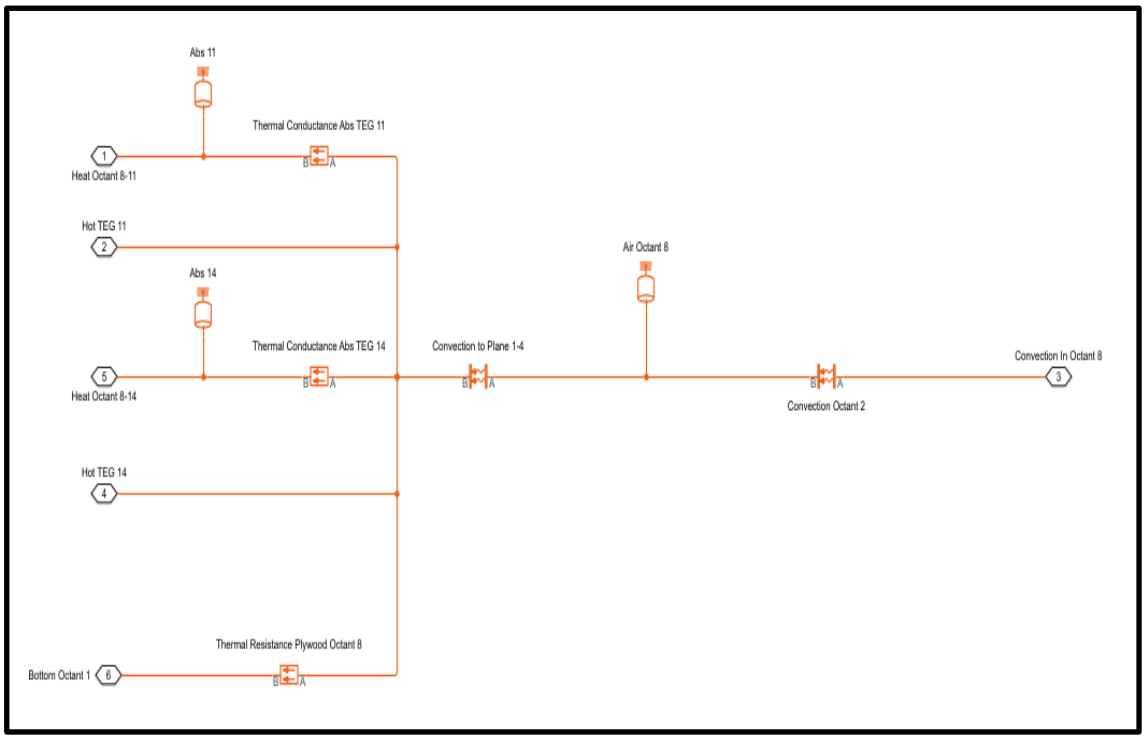

Figure 6. Lower Octant schematic showing Octant 5.

$$0 = \mathrm{H}_{O_{1-5}} \dot{T}_{air} - \left(2k\dot{T}_{teg} + 2k\dot{T}_{abs} + K\dot{T}_{abs}\right) - \left(2\left(\rho cV\right)_{abs} \ddot{T}_{abs} + 2\left(\rho cV\right)_{teg} \ddot{T}_{teg} + \left(\rho cV\right)_{air} \ddot{T}_{air}\right) \quad (6)$$

This relates the input of Octant 5 with the octant geometrically above it which is Octant 1.

3.2.3. Top/Bottom Thermal Resistance loop

This thermal loop has two orientations related to variation of the thermal conductivity. The thermal resistance for the control system will be the same as the bottom thermal conductivity. The bottom surface is built to be geometric symmetrical with the bottom. Below both the insulated surface and non-insulated surface thermal circuits are shown in Figure 7 and Figure 8.

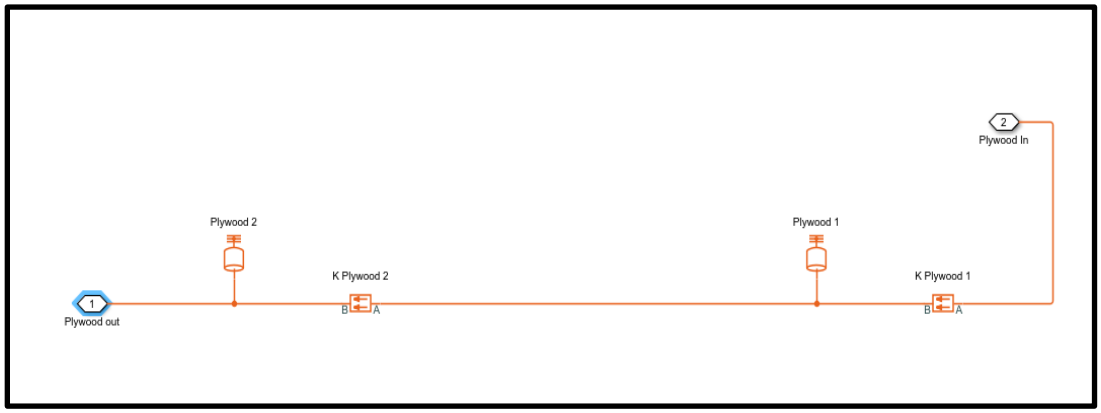

Figure 7 non-Insulated wall thermal circuit

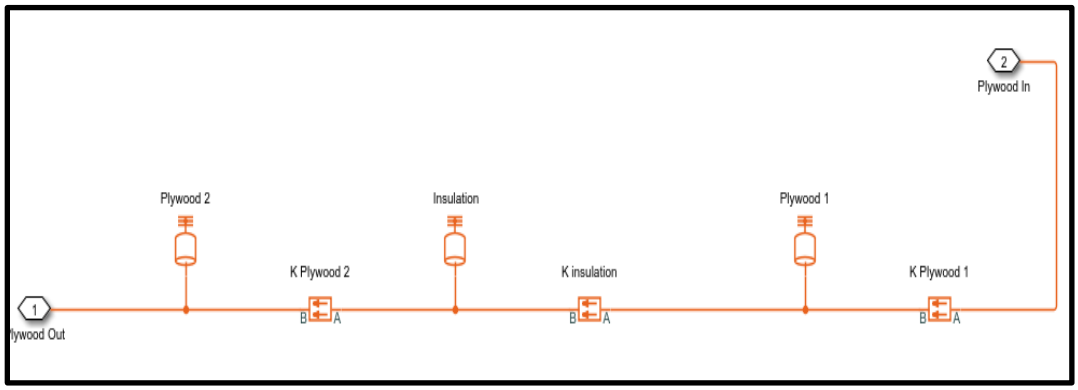

Figure 8. Insulated wall thermal circuit.

This circuit shown while it looks like a simple electrical circuit it is closer in computation to the circuit shown in Figure 9. This circuit acts only through single section of the wall with irregular materials and thus the wall circuitry seen in the following sections will be more detailed. It must be noted that to consider the approach equivalent it must be acknowledged the order of materials physically and the truly complexed interlaced behaviors.

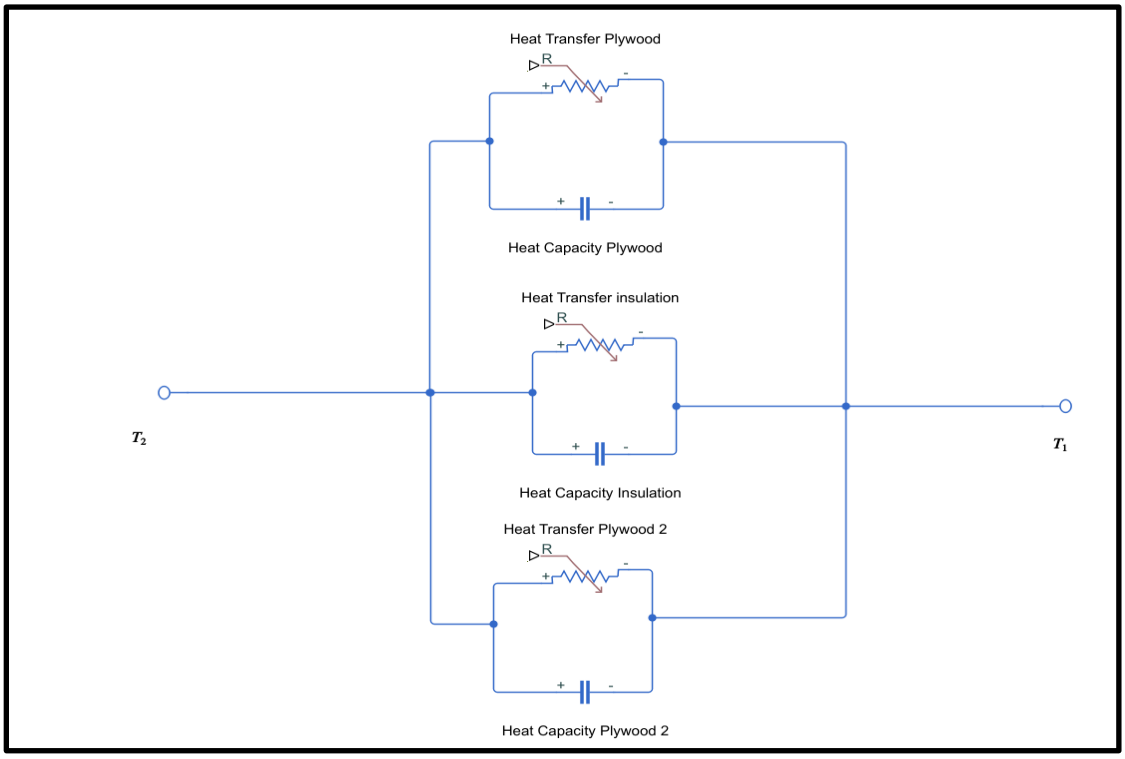

Figure 9. Electrical Equivalent of the thermal circuit

Thus, by performing analysis on the individual loops and then we received the non-homogeneous DE shown below. Where the homogeneous case occurs at the steady state temperature.

$$T_{out} = T_{in} - \left(C_{mat,i}\dot{T} + K_{mat,i}T\right)$$

If the energy balance is performed at each point, the results are

$$T_{out} = T_{in} - \sum_{i=1}^{n}\left(C_{mat,i}\dot{T}_i + K_{mat,i}T_i\right)$$

If the approaches used for the octants analysis are used, then the correlation in equation 7 can be used for the insulated surface. Meanwhile, equation 8 may be used for the bottom surface and the non-insulated.

$$T_{amb} = T_{in} - \left(C_{ply}\dot{T}_{ply,1} + K_{ply}T_{ply,1}\right) - \left(C_{ins}\dot{T}_{ins,2} + K_{ins}T_{ins,2}\right) - \left(C_{ply}\dot{T}_{ply,3} + K_{ply}T_{ply,3}\right) \quad (7)$$

$$T_{amb} = T_{in} - \left(C_{ply}\dot{T}_{ply,1} + K_{ply}T_{ply,1}\right) - \left(C_{ply}\dot{T}_{ply,3} + K_{ply}T_{ply,3}\right) \quad (8)$$

By implementing the heat transfer loop of the material, we can achieve a relationship of heterogenous material shown in equation 9 and 10. This is achieved by assuming the average temperature of the wall surface.

$$Q = \frac{2}{C_{ply}} \dot{T}_{top} + \frac{2}{K_{ply}} T_{top} \tag{9}$$

$$Q = \left(\frac{2}{C_{ply}} + \frac{1}{C_{ins}} \right) \dot{T}_{top} + \left(\frac{2}{K_{ply}} + \frac{1}{K_{ins}} \right) T_{top} \tag{10}$$

3.2.4. Thermal electric conversion circuit

Thermal electric circuit energy balance is somewhat straight forward. First performing the energy balance of a single tile, we can produce the output below given half joule heating electrical loss and thermal conduction. This is shown in equation 11.

$$q = \alpha T_h I - \frac{1}{2} I^2 R + KT \tag{11}$$

$$q = \alpha T_h I - \frac{1}{2} I^2 R + KT$$

Equation too is a meeting of two energy frames and using this relationship produces the electrical power input for each TEG in the electronic circuit.

$$\text{E} = \alpha T_h I_{gen} - \frac{1}{2} I_{gen}^2 R \tag{12}$$

The resulting 16 tile circuit is shown in Figure 10.

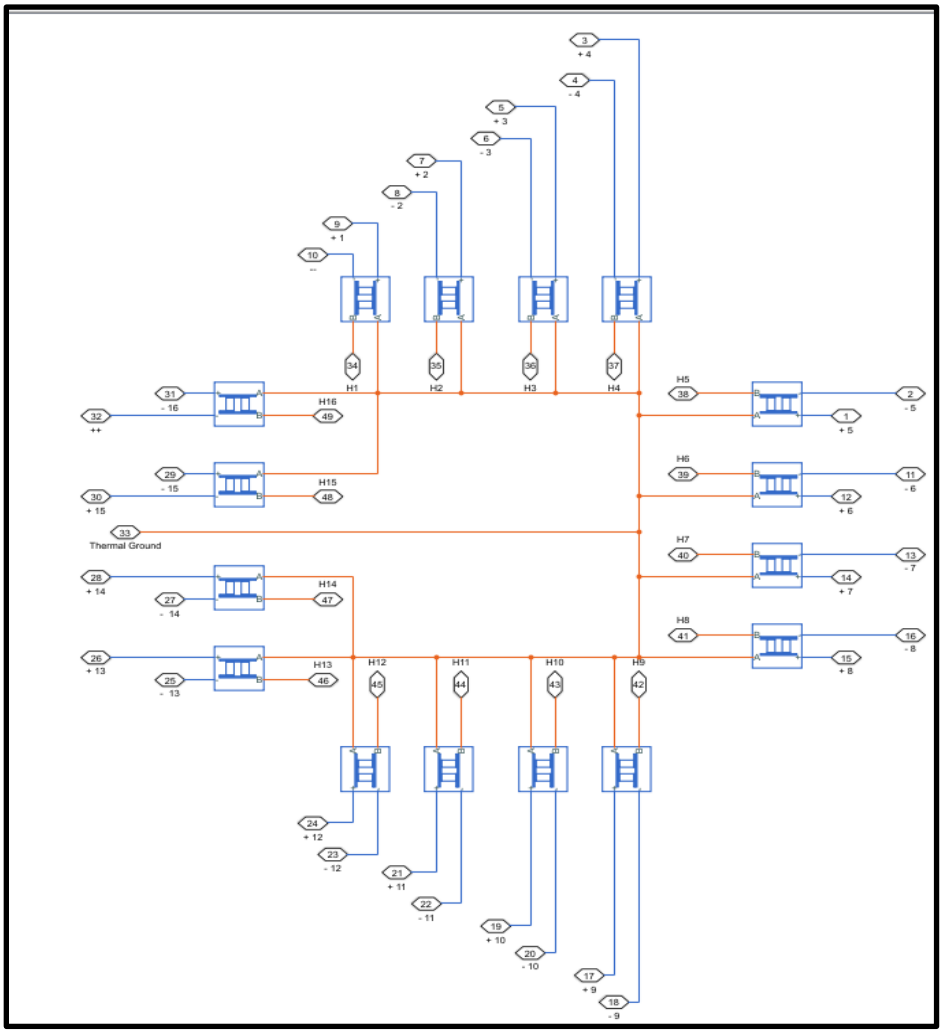

Figure 10. Thermal Electric Conversion Circuit

This circuit because of its uniqueness will be mentioned in the proceeding section to act as a connection between the relationships and the power generation.

3.3. Power Generation Circuit

The power circuit is a simple mathematical optimization. However, this does not indicate that physical optimization will be simple. The case for the project in shown in Figure 11 with a digital drawing of the breadboard circuit shown in Figure 12. The input however, at each node requires consideration of the circuit in Figure 11. This circuit shows batteries powering a circuit and small amount of power is being leached by introducing a large resistor and a diode. This ensures the electrical power will maintain desired polarity. This voltage reading would be captured

in bits and then would be converted to a voltage. This approach does require dampening to ensure that 5 V maximum is not achieved. The voltage drop can be recovered by considering it in the voltage calculation performed by the microcontroller. This creates a potential for error that must be acknowledged. The way the system is designed if the system deviates in any way from the standard operation, then the microcontroller would need to be programmed with the new values initialized.

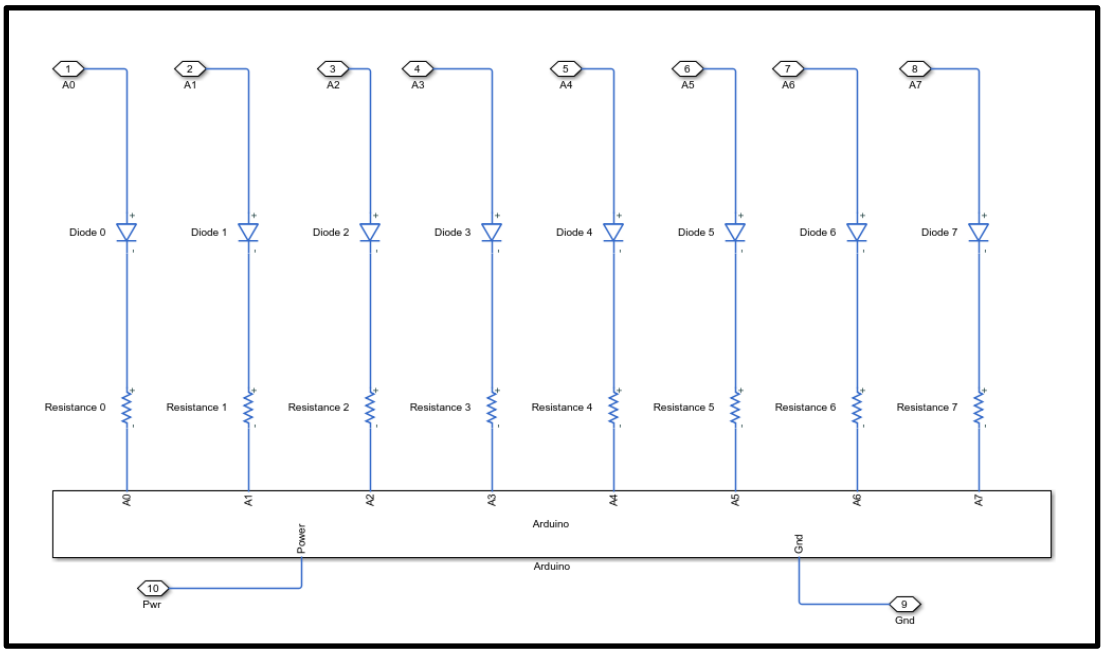

Figure 11. Arduino Circuit Drawing

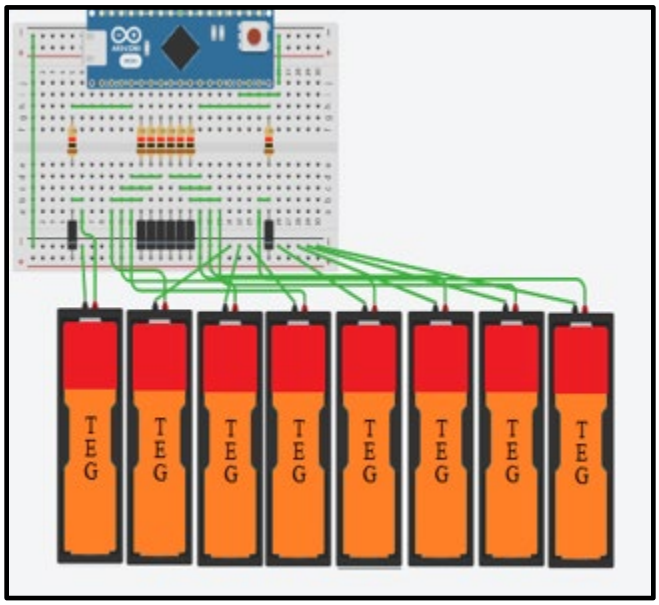

Figure 12. Digital Drawing of the Arduino circuit connected with the TEGs

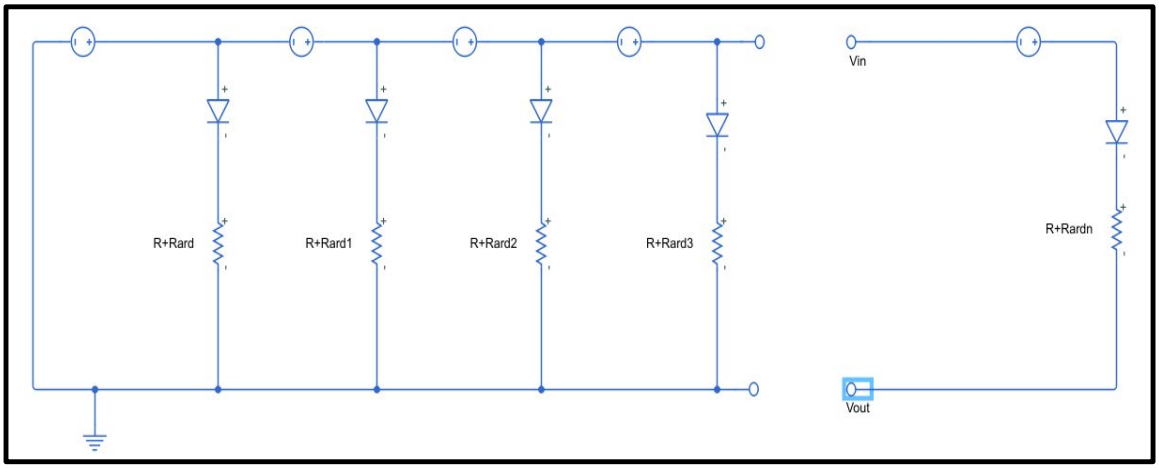

Figure 13. TEG circuit diagram

The results of balancing the loops of the electrical circuit are shown below. This implies that after the first voltage each proceeding voltage must be diminished to appropriately measure the voltage produced. This is shown in equation 13.

$$\Delta P = (VI)_{teg,i} - \frac{1}{2}(I_i)^2 R_i \qquad (13)$$

Using the standard loop law this equation represents the power dissipation or generation at the various nodes. The reason this will helpful is it will achieve our power outputs for each TEG cell quickly. There is one set of considerations be made to appropriately optimize the circuit. These considerations are shown below.

$$R_n < R_{n-1} < \ldots R_2 < R_1$$

This allows the circuit to seep the circuitry and overlay loops to perform further optimization. This would be done by tuning the combined circuitry at the various nodes of interaction. To avoid such complication the standard of large and progressively smaller resistances is used with the final resistance minimized to maximize the power dissipation at the load resistor.

3.4. Combined system

The combined system while maintaining a number of relationships, was simplified in the previous section to create common variables. These common variables would be represented to values related to the energetic interactions. These energetic actions have behavior based on the material properties.as long as each node is considered to be approaching some convergent point. Thus, the bias array will be represented by the various coefficient for each variable. This can then be used to compute the values of each measurement and was necessary in the setup of the manipulation of the data collection systems. Each node is assumed to converge on common nodes. The common nodes are the heating element power rating and the ambient air temperature. approaching some convergent point. Thus, the bias array will be represented by the various coefficient for each variable. This can then be used to compute the values of each measurement and was necessary in the setup of the manipulation of the data collection systems. The combined

system shown in Figure 14 (page 21) show the connections of the various components. Figure 15 (page 22) shows the expanded unique components.

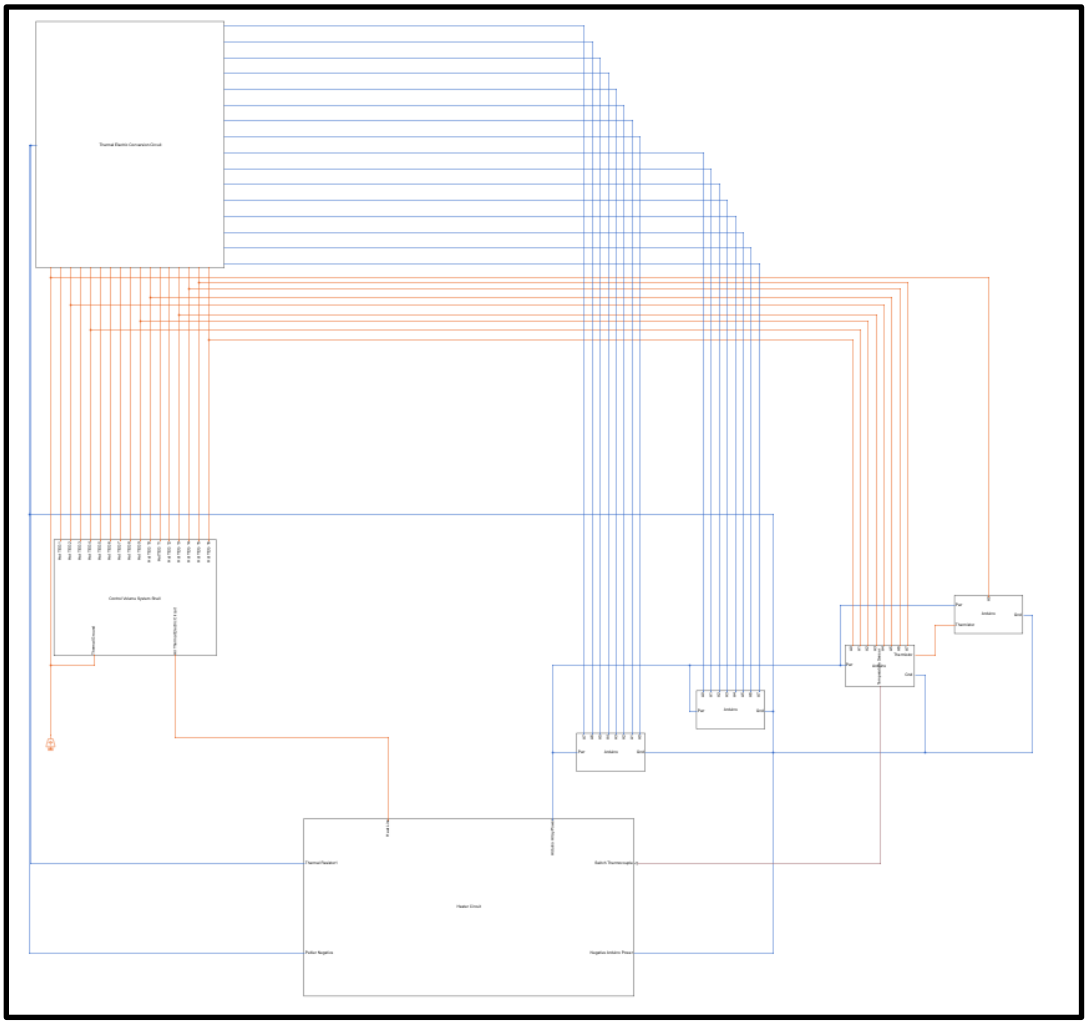

Figure 14. Full Thermal Electric Circuit

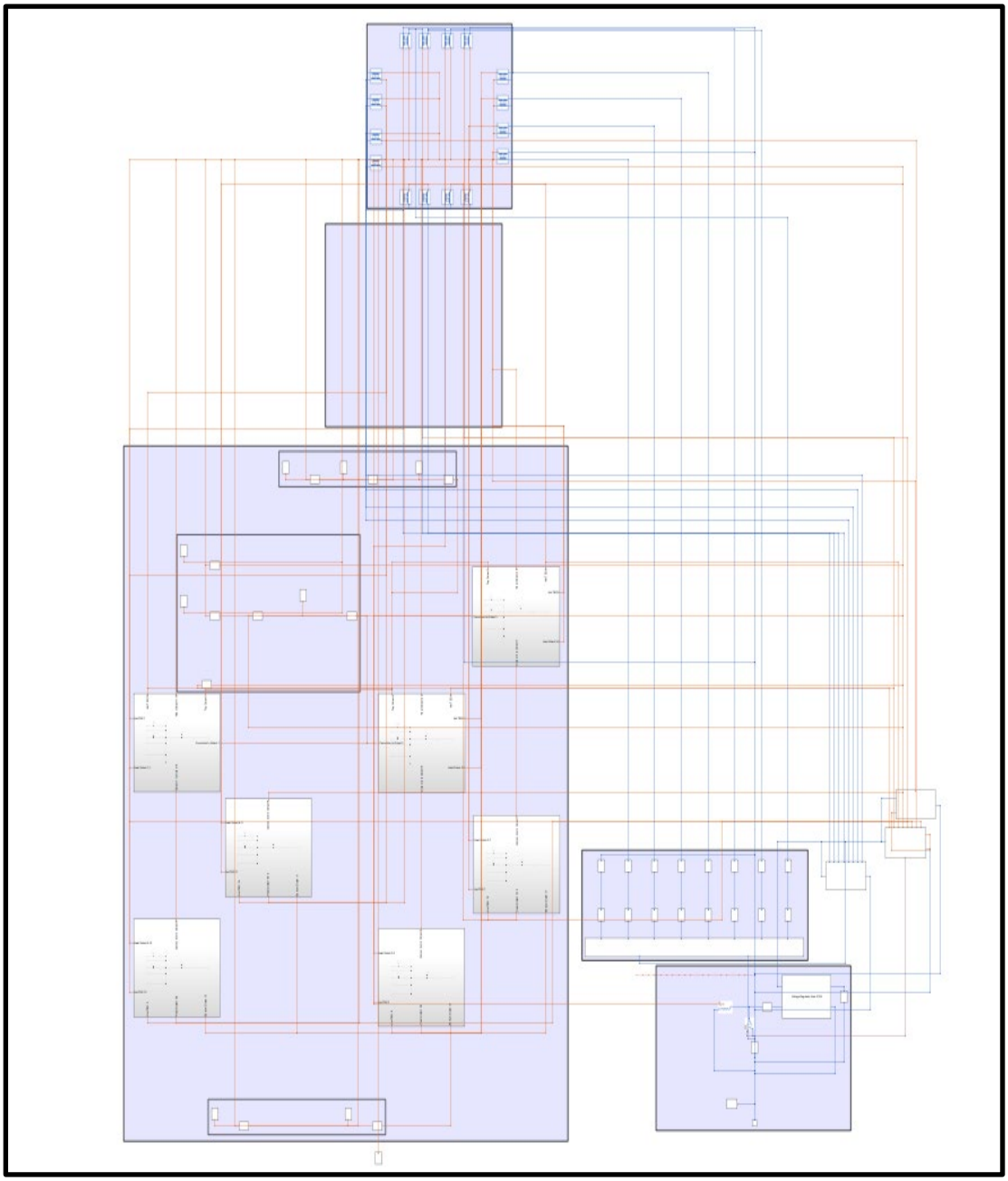

Figure 15. Full Thermal Electric Circuit with expanded components

4. **Experimental System**

The initial experimental system is not covered due to a more accurate and a system that could be more easily tracked. This completed system no insulated system shown in Figure 16 and the insulated system shown in Figure 17 (page 22). The chamber is heated and all electronics capturing the system are going through the simple circuit from Figure 12 with the batteries marked TEG representing the thermoelectric components. The components can be seen in Figure 16 Labeled TEC1-12706.

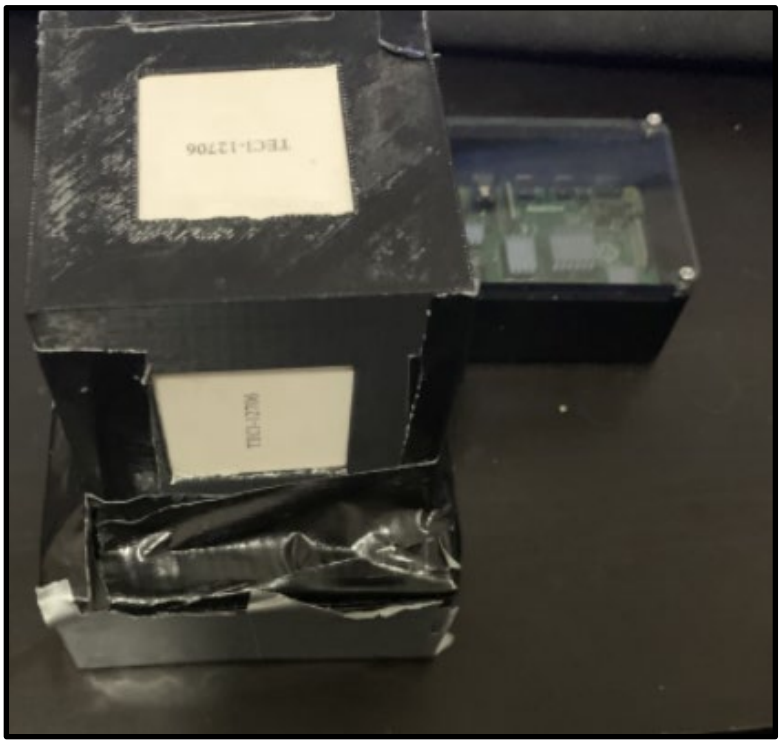

Figure 16. Non-Insulated System

This smaller system was designed after some unforeseen data noise was experienced in the previous datasets. This simplifies each wall to be small enough to be treated as individual cases.

The Thermal Electric Circuit for each wall is shown in Figure 18. The general premise from system 1 and system 2 is the flux proportions themselves are being manipulated. Thus, if the flux is decreased through the top of the system some of the flux will be stored and provide a new set of steady state conditions, however, the power increase is predicted to be disproportionate to the temperature increase. The system operates simply by plugging in the power. The system as been tuned to prevent temperature that are too high and are explicitly meant to explore the phenomenon.

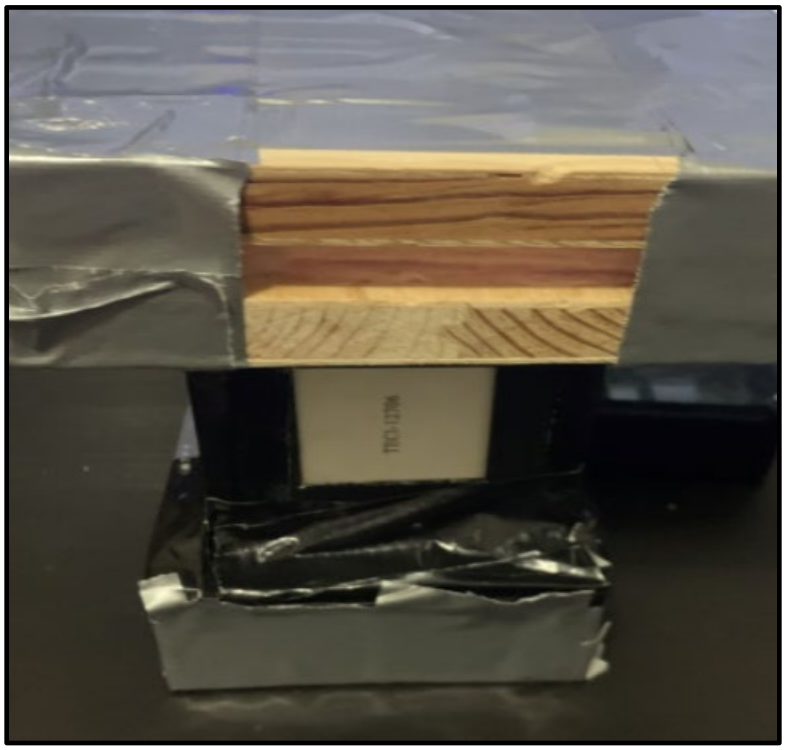

Figure 17. Insulated System with Material Showing

5. Simulations

To avoid difficulty associated with the computations, SIMULINK, a simulation software, was utilized to perform the two test cases. This was done to verify the theoretical observation made. This allows for a quick performance test to ensure that the cases can hold true and that the changes will influence the way the heat flow occurs.

5.1. Simple Simulation

The simulated system involved tuning related to the circuit relationships. As was shown in equations 1-12 (pg. 10-20) there is a connection between tuning the thermal conductivity and the electrical resistance to achieve an optimum. This difficulty was not previously observed due to the control volume being centered around the TEG. This proved quite a challenge. The reason for this is the simulation was considered at a steady state. Therefore, the complete behavior is not observed until the transience in the fluid is accommodated, as well as the tuning the resistance. To reduce this complexity is impossible with standard resistance values, and more advanced circuitry knowledge would be needed to fully address this obstacle. A picture of the test cases and only optimized electronics are shown in Figure 18 (page 24).

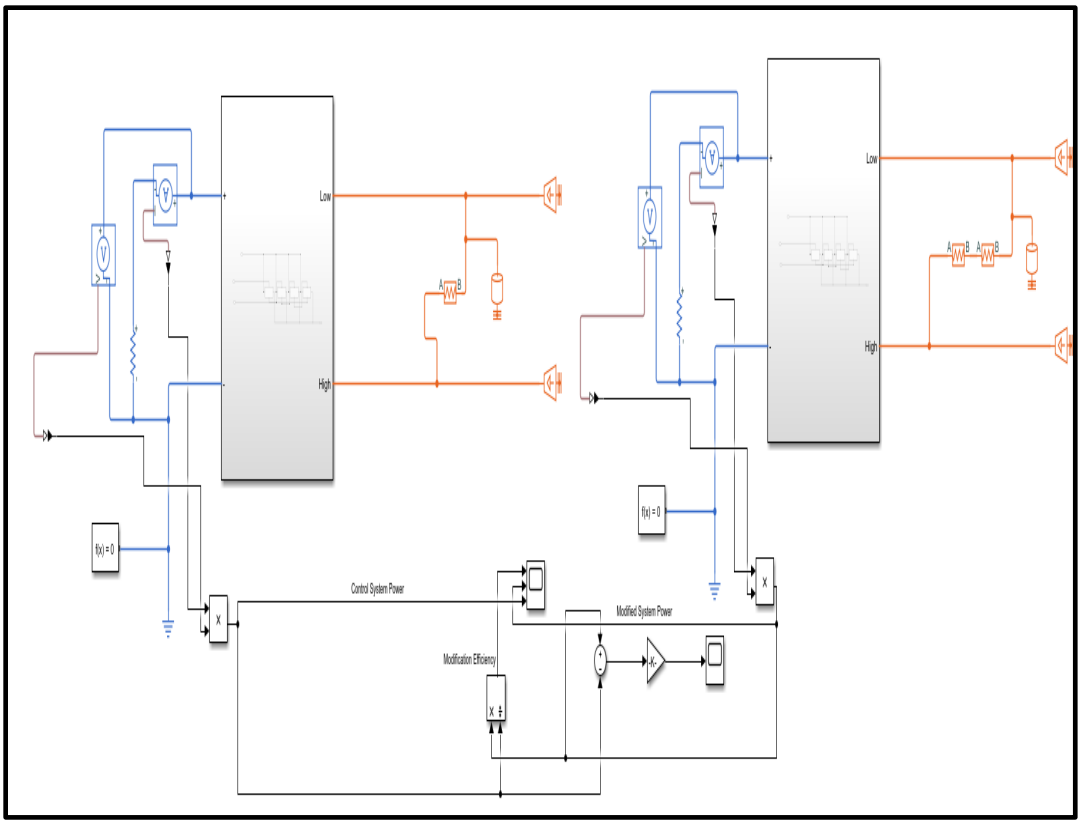

Figure 18. Simulation Set-up of Standard System(left) and Modified Insulated System(right).

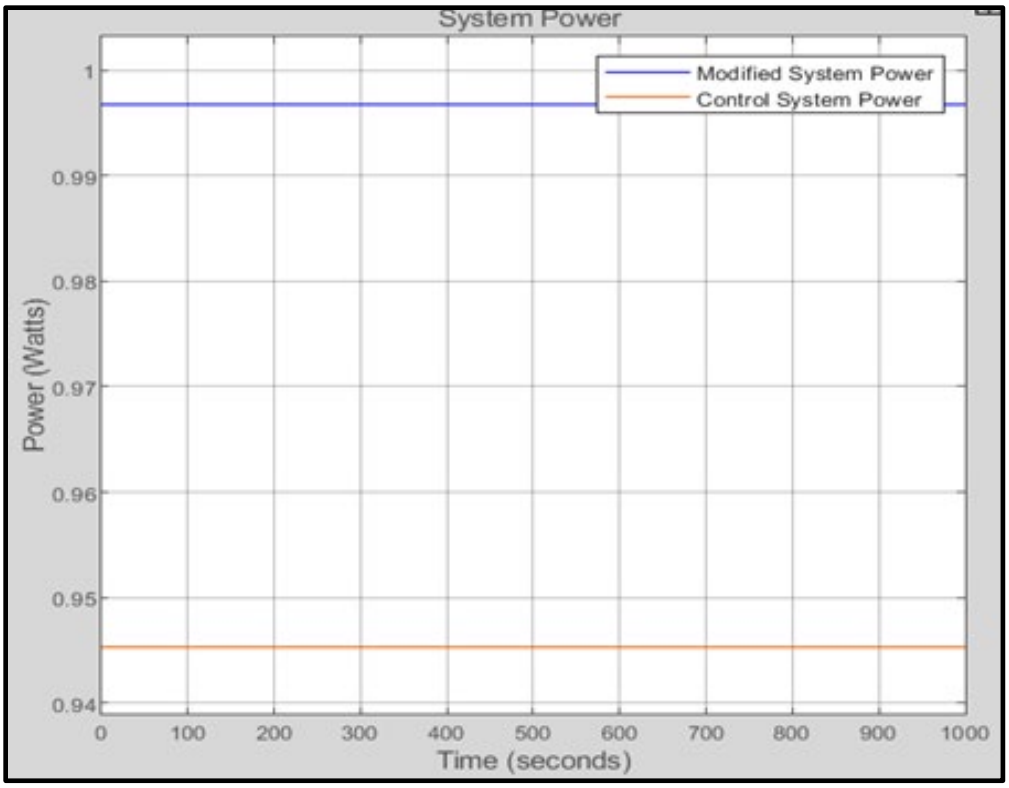

Figure 19 The simulated Steady State Signal of both Case 1 and Case 2

The left side of Figure 19 (pg. 24) is a single element and would symbolize the standard system with cladded insulation system. If not correcting for the presence of the TEGs, the system will operate at a lower temperature based upon this test. In Figure 19, the modified system that uses insulation on the side. This should increase the internal temperature which would show an increase in the internal energy. This would be easiest to see by observing if there is a power increase. These are based on a steady state operating condition. The simulation results at steady state conditions shows an improvement in the simple system of just over 5%. This outcome justifies an additional physical experiment to confirm practical application.

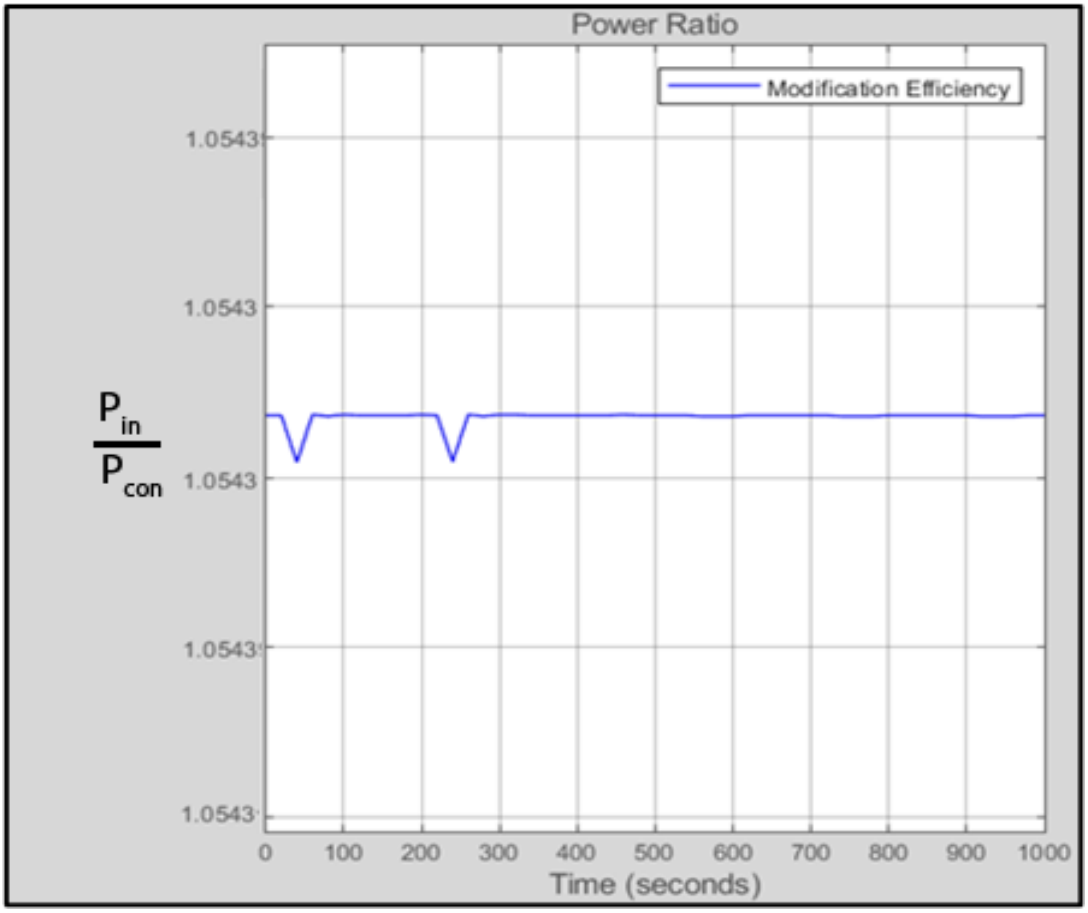

Figure 20 The efficiency change based on the system being utilized.

This also proved to be the case with the more complicated mixed circuit. The values however are lower by an order of magnitude with convective forces at $h = 5\frac{w}{m^2 \cdot k}$. The approximate mixed circuit power values typically resulted in a maximum 70 mW of recovery per tile on average and reached up to 105 mW for the more advanced system. The maximum power increase was about 5%. This was based upon the utilization of a temperature controller to create an oscillating heat load on the thermal volume.

5.2. Simulation Based on Redesign

After receiving feedback from the initial design, a new simulation shown in Figure 21 on page 26 can be seen. This simulation was produced to confirm the value received by the data

collection in the newer simplified system. The approach was the same limit heat flux through the individual tile cells. This simulation set up is shown below. This is for the non-Insulated set up with only the thermal resistance value varying across the two systems.

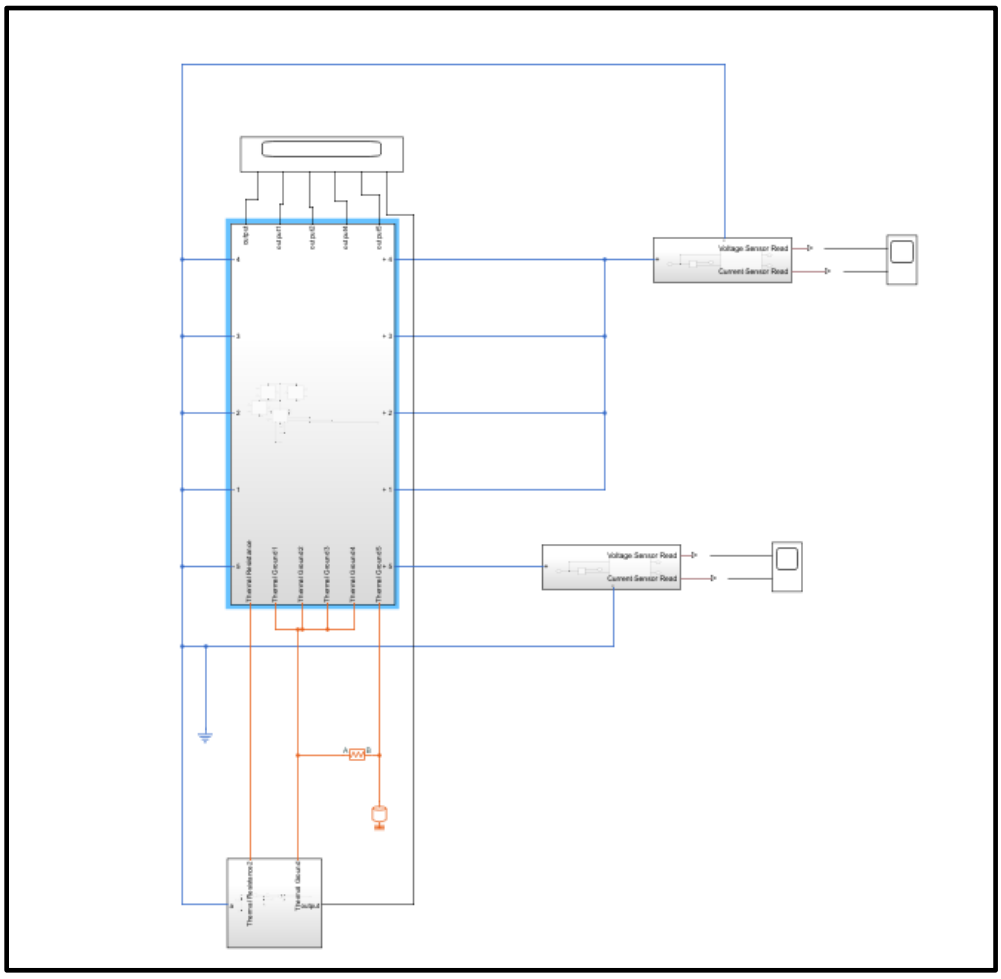

Figure 21. Redesigned Simulation Setup

After running the simulation, the top wall TEG was tracked separately as the case for power reduction and the all the other tiles contribute to power. The results in Figure 22 and Figure 23 show the Voltage over time graphs. These graphs indicated that power in the insulated-tile cell in the insulated system and the non-insulated system. Comparatively, it can be seen that

the insulated system does successfully add dampening to the thermal system at that node by making an exchange of fluxes.

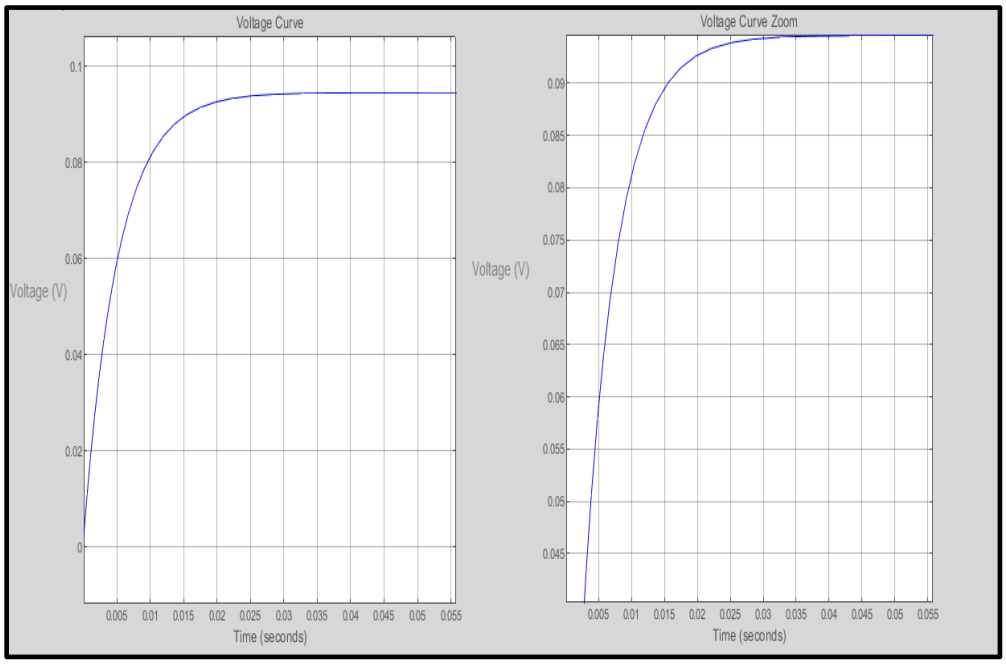

Figure 22. Tile Non-Insulated System

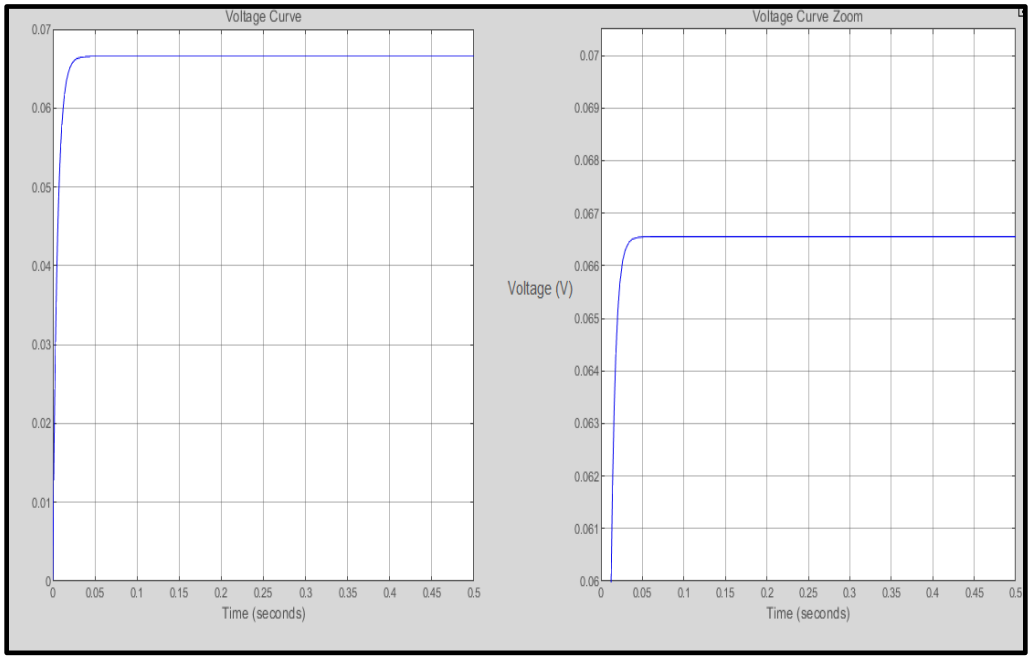

Figure 23 Tile Insulated System

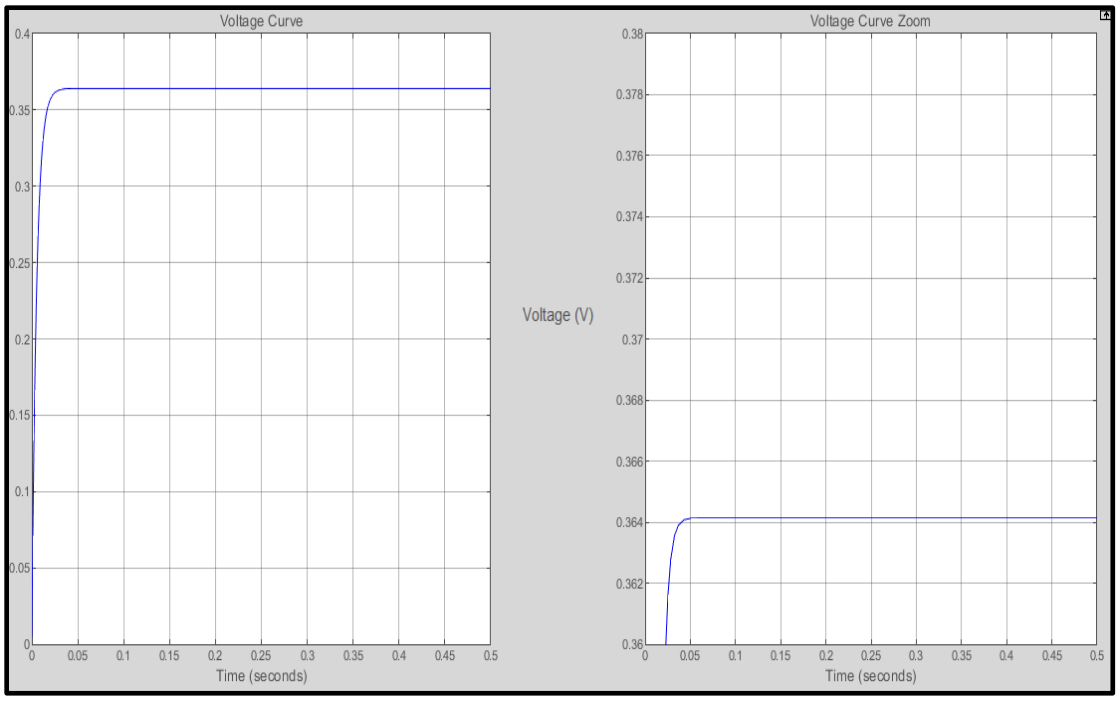

Figure 24. Non-Insulated System

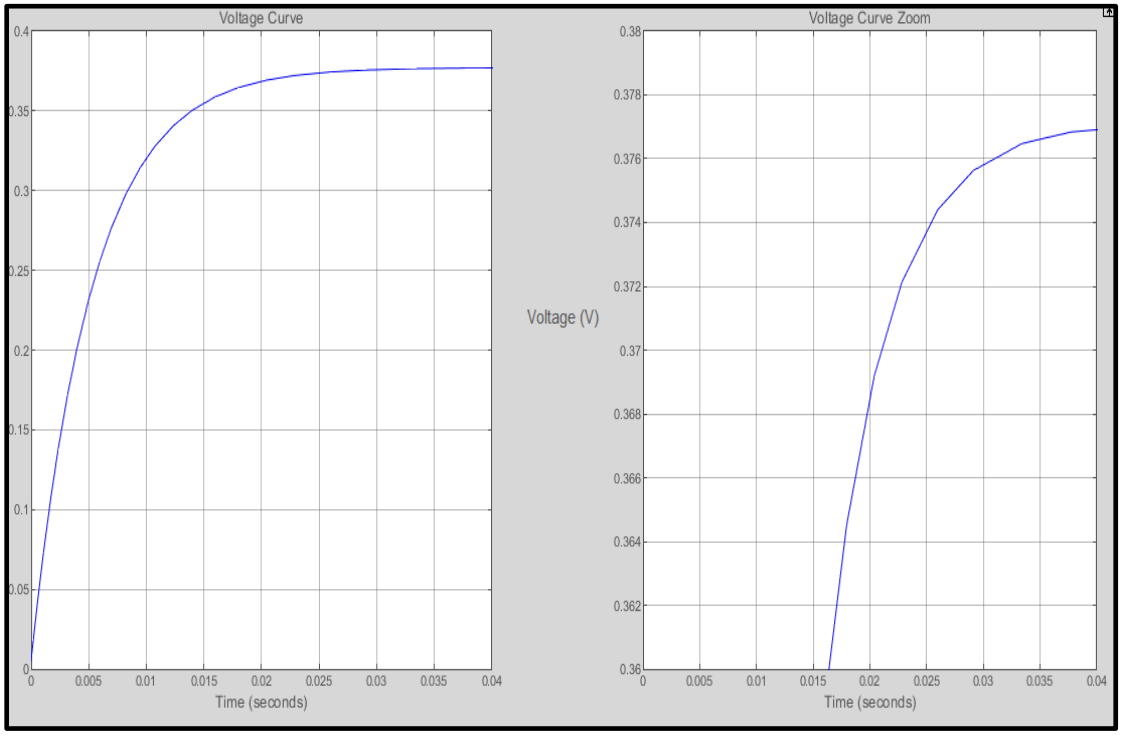

Figure 25. Insulated System 4 Cell Voltage Production

In Figure 24 and 25, the flux has been shown to decrease through the top TEG, and now the voltage increase phenomenon is observed. The temperatures internally at each node were tracked and are all the same. Thus, under normal conditions should produce the same power for each tile. In other words, the single tile should be exactly ¼ of the total given by the second node being measured. This has been shown to be false and a new physical system tracking was necessary.

6. **Experimental Results**

Using a data logger, the internal and external temperature was tracked, and the electrical power generation of each tile was measured. The average internal temperature of the system was tracked using several data sets, and these sets performed consistently with only slight data noise. The noise in the data set was permitted due to small quantities being computed, in order to mitigate the prediction that the data sets would unreasonably smooth. In Figure 26 and Figure 27 (pg. 31) the resulting plots of a random sample was generated from the data sets of three hours of 0.25 second time steps.

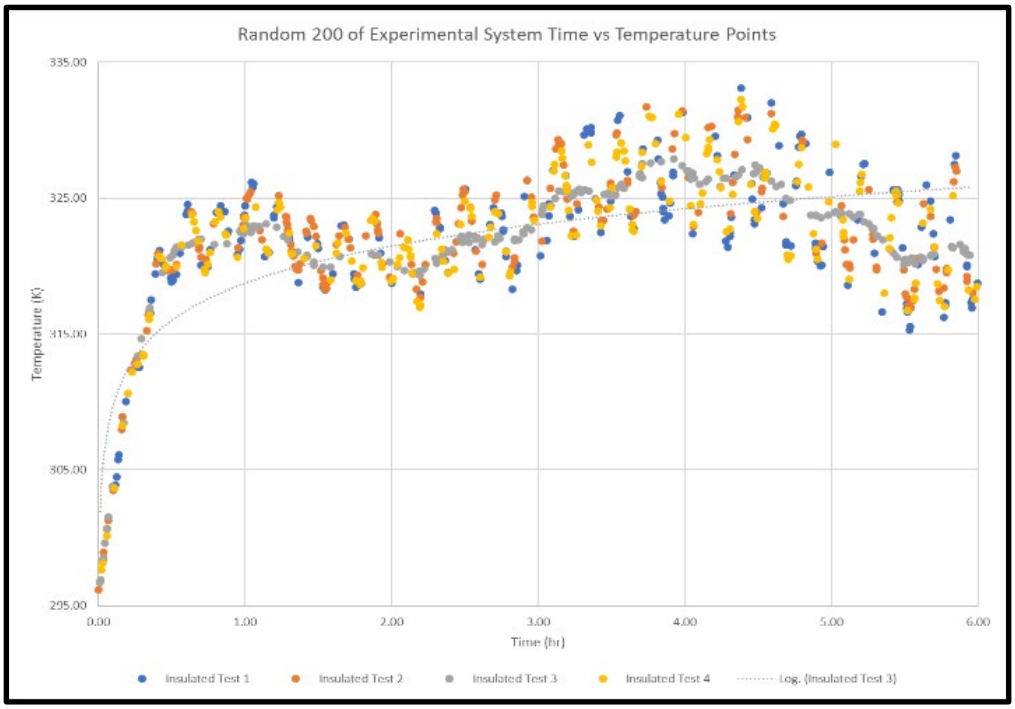

Figure 26. Insulated System Temperature Plot

The purpose of the energy relationship is to ensure an increase in energy along with the increase in power. This implies that we increase the heat flux through the TEG array while reducing the energy losses to surroundings.

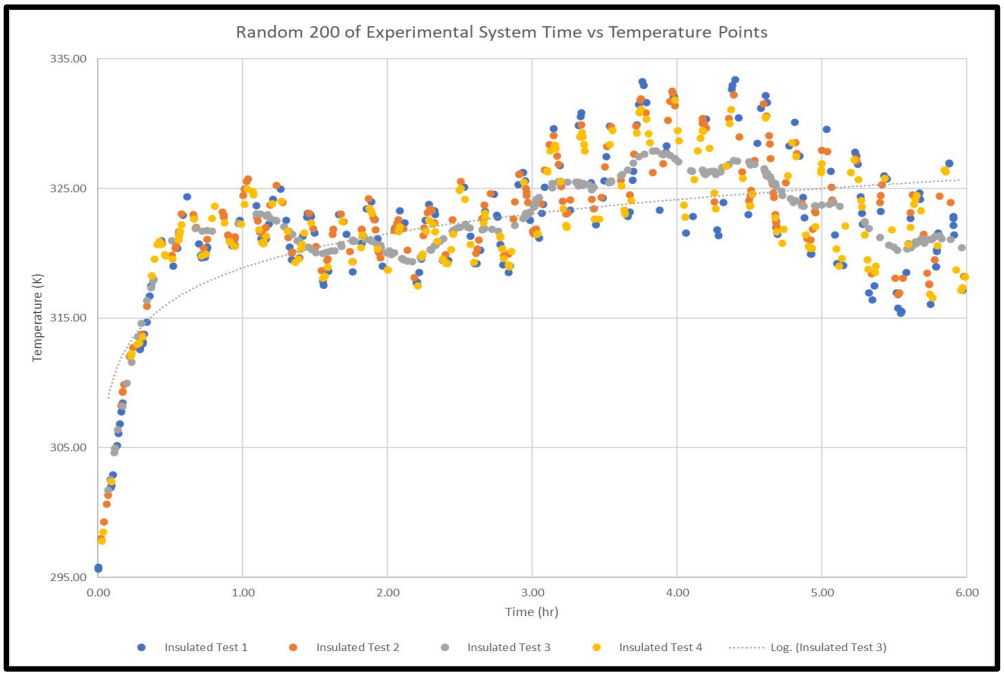

Figure 27. Control System Temperature Plot

Then by using the material properties[9][3][6] shown in table 1 above, and the geometric properties shown in table 2 (pg. 32),

Table 1 Material Properties of the System[9][3][6]

Material	**k** $\frac{w}{(m^2 \cdot k)}$	**ρ** $\frac{kg}{m^3}$	**V** m^3	**A** m^2	**C** $\frac{kJ}{(kg \cdot k)}$
ABS	0.175	0.232	6.74E-04	0.0071	1.17
TEG	0.175	770	6.27E-06	0.0016	0.15
Insulation	0.63	0.98	4.24E-03	0.00016	0.81
Plywood	0.833	0.420	4.24E-05	0.0167	1.20
Air	26.1	1.15	1.98E-03	0.0144	0.72

Table 2. System Geometric Properties

Wall										
Basic Shape				**Hole**				**Dividers**		
Height	Width	Thickness		Height	Width	Thickness		Height	Width	Thickness
129.2	129.2	9		39.6	39.6	9		40	20	7
Area	Quant	Volume		Area	Quant	Volume		Area	Quant	Volume
Area						Volume				
Wall	Air	Tile	Divider	Net ABS		Wall	Air	Tile	Divider	Net ABS
0.016693	0.014448	0.00156816	0.0008	0.007093		0.00015	0.001978	6.27E-06	1.6E-06	0.000131

by tabulating the change in energy over time, a measurement of the relationship between power and internal energy can be observed.

This internal energy is proportional to the temperature, and the power is proportional to the temperature difference across the boundary. Careful observation reveals that the experimental system has an internal energy that trends higher (i.e., has a higher temperature). A condition for application is that in our case the system energy trend must be higher. Thus, this confirms the condition has been met.

To track that models' performances of the individual models, the power plots were generated and then a logarithmic regression line was found for each. The distance between the logarithmic regression lines would indicate an effect caused by the approach. It can be seen the results provide a divergence from the standard power generation of Case 1, shown in Figure 28 (pg. 23). The comparisons of the early transience power generation are also shown in Figure 29 (pg. 23). This looks similar to Figure 1 (pg. 3), which helps verify that the system is generating power properly. The value at peaks shows a ~40mW and ~50mW for Case 1 and Case 2, respectively.

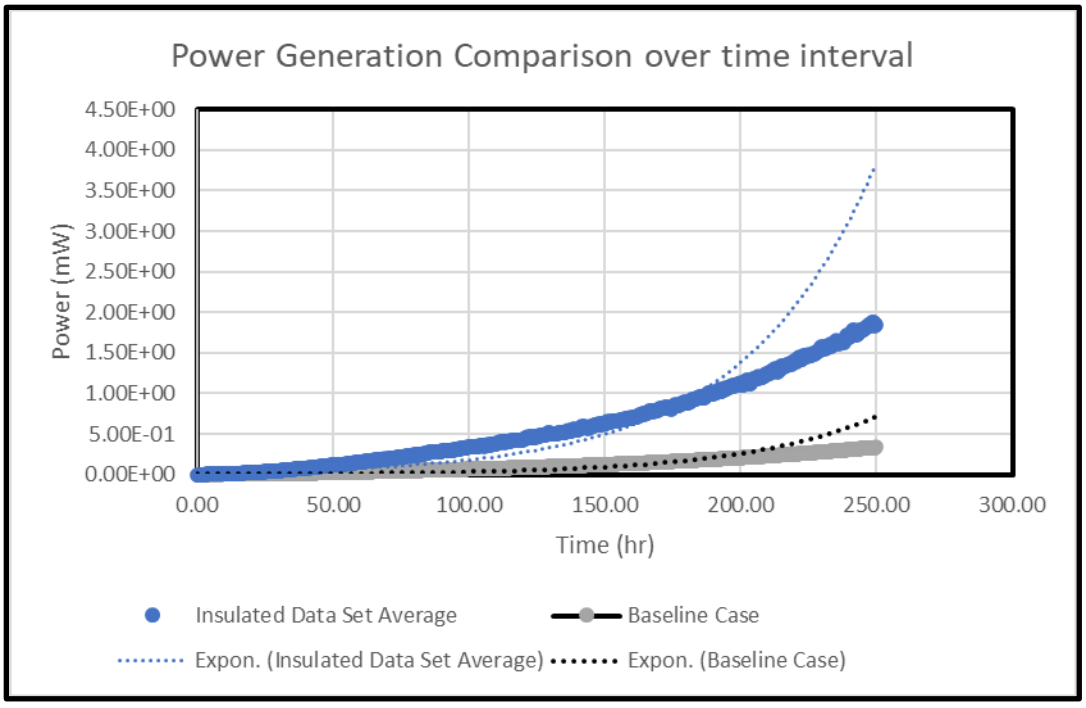

Figure 28. Power Generation of Case 1 and Case 2

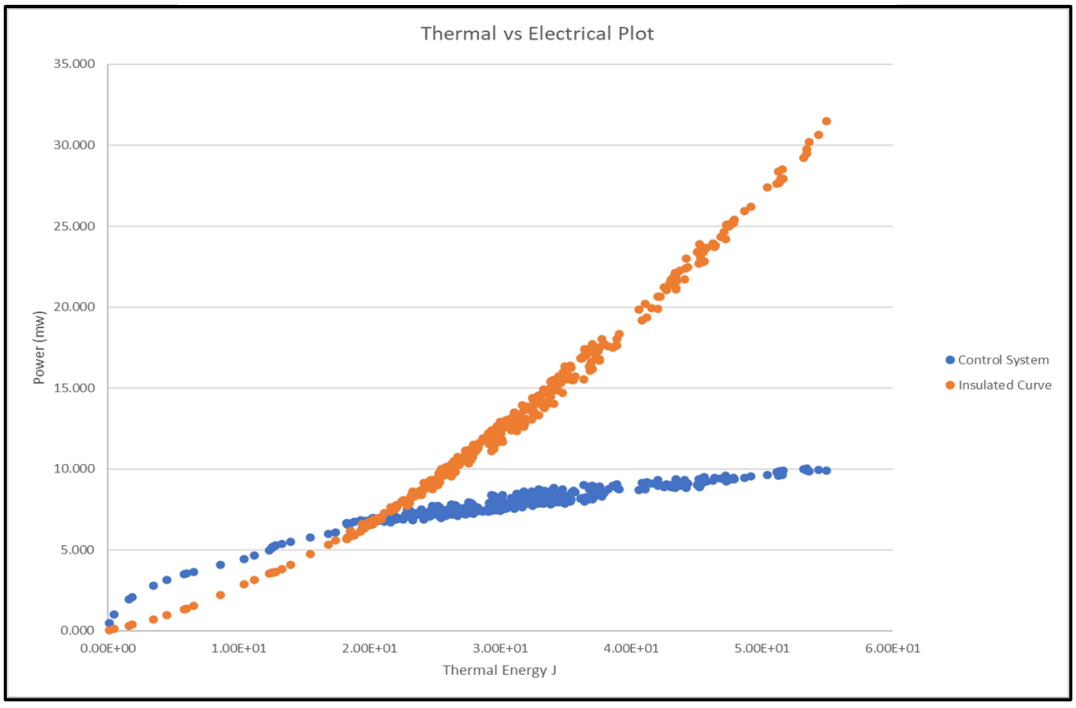

Figure 29. Power Graph for Transient Conditions

While our initial data set was promising it showed some slight concerns. These concerns were rectified by simplifying the phenomenon present in the system. These restrictions used

methods such as a smaller air cavity and more physical contacts where air gaps are present. The data, plotted in Figure 30

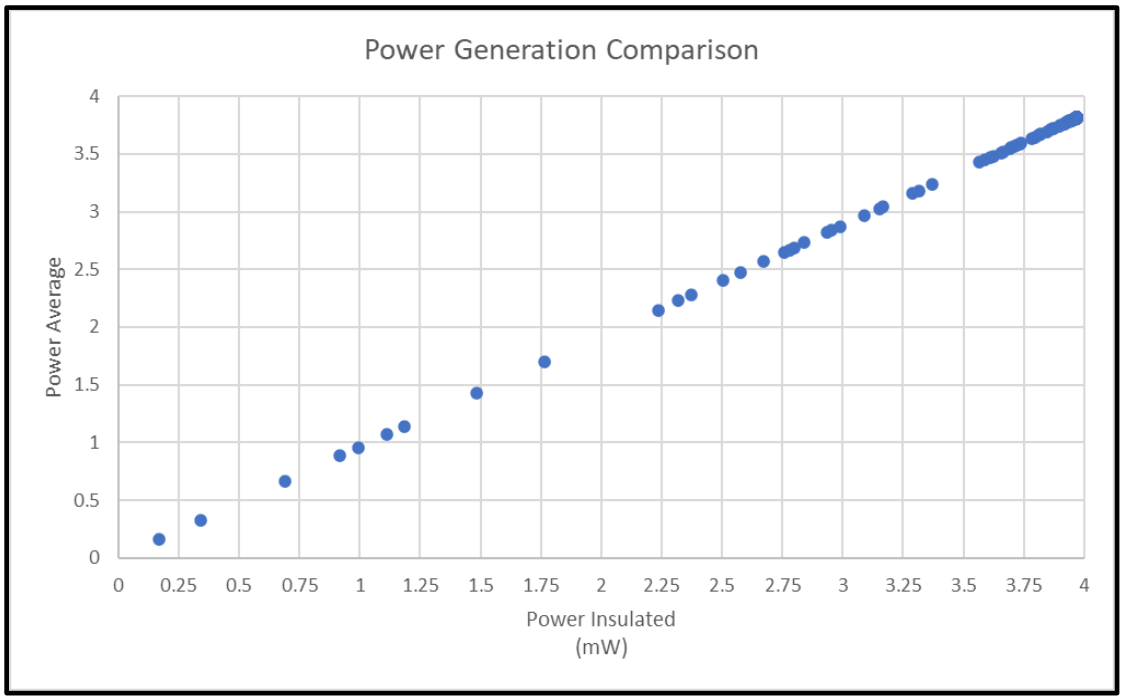

Figure 30. Power TEG 1 Cell Versus Insulated TEG

correlates the power generations of the system. This in fact does show a strong correlation in the change and the power production, however, it is not a one-to-one change and thus confirms the hypothesis. This power production appears to be a linear increase as function of power which is a function of temperature. However, the internal temperatures of the system are almost identical and thus we can neglect the temperature driven heat exchanges and thus conclude the flux changes are the primary increase.

These relationships are shown through time using the simplified system in Figure 31. The results show a power production difference in the new tile element while them temperatures are the same. This supports the hypothesis that redirecting the heat rather than preventing it entirely might be a more useful endeavor.

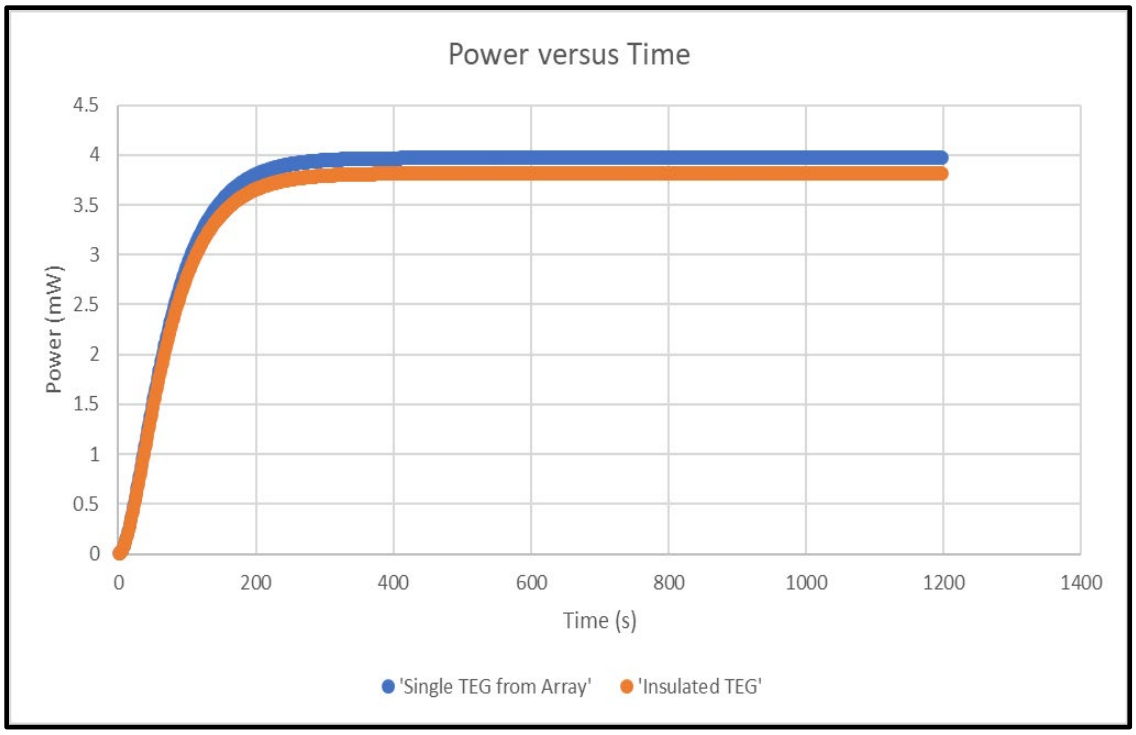

Figure 31. Power Generation TEG Cell - 1 Tile Versus Insulated Tile through Time

7. Conclusions

Based upon the initial data sets and the theoretical considerations, the hypothesis appears to have a basis in practical application. However, because the data was a little bit abnormal and given the low values a new set of tests was conducted while considering the flow through a specific region and whether or not it could be shown to be increased. These results were shown to have a positive correlation.

This had some behavior that was not foreseen and thus a new approach was considered which simplified much of the potential complications. This simplification shows a change in the behavior that is not one to one and thus it can be stated that there seems to be some benefit. Further research could be done to optimize the various parameters and sizes to discern the ration of cladding to tiles and the optimum quantity of power producing regions. This would require a parametric study of large magnitude to fully take advantage of this particular design.

The initial assertion has been met. The many obstacles throughout the course of the research made certain approaches unachievable in the given span of time. The outcome shows a small increase of power across all tiles and each tile receives a small percentage of the losses experienced from the insulated side. This resulted in a list of several design concerns that could be added to, or modified, to improve the concept. One consideration would be to promote additional heat transfer through the generators using a heat sink on the TEGs. Another approach, that is much harder given limited experience,

involves tuning the electric circuit to synchronize with the heat transfer direction and magnitude such that the thermal resistance equivalent is equal to the thermal circuit. This would be achieved by using air flow sensors connected to a switch designed to modify the resistance value based upon the local air velocity. The final consideration is designing a system that makes full use of all fixtures, such as walls, pipes, burnout valves, and any other fixture that emits heat and can have a TEGs practically integrated with it. This research hopes to give groundwork for more complex cases for future research. These complicated cases could involve highly advanced and versatile TEGs, such as flexible TEGs[15], micro[9], and nano[5] TEGs. These advanced devices would allow for the optimization of the ratio of generators versus insulation. Thus, using TEGs and thoughtful thermal fluid design in a highly versatile electrical system can be achieved.

8. **Reference**

[1] H. S. Lee, *Thermal Design: Heat Sinks, Thermoelectrics, Heat Pipes, Compact Heat Exchangers, and Solar Cells*. 2010.

[2] Chen; Meng, "'The Deep Sea Water and Heat Energy of Thermoelectric Generation Study,'" *Electrochem. Soc.*, 2015.

[3] B. I. Ismail and W. H. Ahmed, "Thermoelectric power generation using waste-heat energy as an alternative green technology," *Recent Patents Electr. Eng.*, vol. 2, no. 1, pp. 27–39, 2009, doi: 10.2174/1874476110902010027.

[4] H. Lee, *Thermal Design: Hear Sinks, Thermoelecrtrics, Heat Pipes, Compact Heat Exchangers, and Solar Cells*, 1st ed. Hoboken, New Jersey: John Wiley and Sons, Inc, 2010.

[5] R. D.M., *Thermoelectrics Handbook: Macro to Nano*. 2010.

[6] X. F. Zheng, Y. Y. Yan, and K. Simpson, "A potential candidate for the sustainable and reliable domestic energy generation-Thermoelectric cogeneration system," *Appl. Therm. Eng.*, vol. 53, no. 2, pp. 305–311, 2013, doi: 10.1016/j.applthermaleng.2012.03.020.

[7] S. Naher, D. Orpen, D. Brabazon, C. R. Poulsen, and M. M. Morshed, "Effect of micro-channel geometry on fluid flow and mixing," *Simul. Model. Pract. Theory*, vol. 19, no. 4, pp. 1088–1095, 2011, doi: 10.1016/j.simpat.2010.12.008.

[8] *Heat convection*, vol. 44, no. 04. 2006.

[9] E. Mu, G. Yang, X. Fu, F. Wang, and Z. Hu, “Fabrication and characterization of ultrathin thermoelectric device for energy conversion,” *J. Power Sources*, 2018, doi: 10.1016/j.jpowsour.2018.05.031.

[10] Y. M. Zuev, “Nanoscale Thermoelectric Energy Conversion,” *PhD. Diss.*, pp. 1–33, 2011.

[11] Adminstrator, “Different Types of Diodes: Their Circuit Symbols & Applications.” .

[12] H. Fan, “Design tips for an efficient non-inverting buck-boost converter,” *Analog Appl. J.*, vol. 3, pp. 20–25, 2015, [Online]. Available: https://www.ti.com/lit/an/slyt584/slyt584.pdf?ts=1607342904526&ref_url=https%253A%252F%252Fwww.google.com%252F.

[13] B. Hauke, “Basic Calculation of a Boost Converter’s Power Stage,” *Texas Instruments, Appl. Rep. Novemb.*, no. November 2009, pp. 1–9, 2009, [Online]. Available: http://scholar.google.com/scholar?hl=en&btnG=Search&q=intitle:Basic+Calculation+of+a+Boost+Converter’s+Power+Stage#0.

[14] H. Lee, “Appendix E: Thermoelectric Properties,” *Thermoelectr. Des. Mater.*, pp. 391–398, 2016, doi: 10.1002/9781118848944.app5.

[15] C. S. Kim *et al.*, “Structural design of a flexible thermoelectric power generator for wearable applications,” *Appl. Energy*, 2018, doi: 10.1016/j.apenergy.2018.01.074.

[14] The Online Materials Information Resource. (n.d.). Retrieved January 22, 2021, from

http://www.matweb.com/search/DataSheet.aspx?MatGUID=3a8afcddac864d4b8f58d 40570d2e 5aa&ckck=1.